Molecular Mechanism of Cellular Oxidative Stress Sensing by Keap1

著者	Takafumi Suzuki, Aki Muramatsu, Ryota Saito, Tatsuro Iso, Takahiro Shibata, Keiko Kuwata, Shin-ichi Kawaguchi, Takao Iwawaki, Saki Adachi, Hiromi Suda, Masanobu Morita, Koji Uchida, Liam Baird, Masayuki Yamamoto
journal or publication title	Cell Reports
volume	28
number	3
page range	746-758
year	2019-07-16
URL	http://hdl.handle.net/10097/00128418

doi: 10.1016/j.celrep.2019.06.047

Article

Cell Reports

Molecular Mechanism of Cellular Oxidative Stress Sensing by Keap1

Graphical Abstract

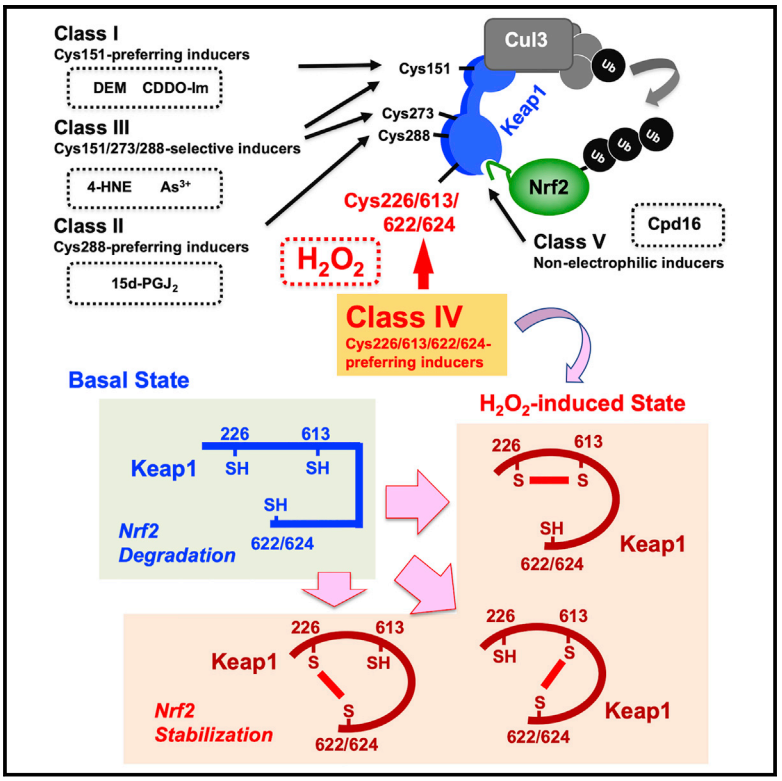

Highlights

- Keap1 H_2O_2 sensor is distinct from that used for sensing electrophilic inducers
- Keap1 uses Cys226, Cys613, and Cys622/624 residues to sense H_2O_2
- Keap1 uses these cysteine residues to set up an elaborate fail-safe mechanism

Authors

Takafumi Suzuki, Aki Muramatsu, Ryota Saito, ..., Koji Uchida, Liam Baird, Masayuki Yamamoto

Correspondence

taka23@med.tohoku.ac.jp (T.S.), masiyamamoto@med.tohoku.ac.jp (M.Y.)

In Brief

The Keap1-Nrf2 system plays a central role in the oxidative stress response. Suzuki et al. show that the H_2O_2 sensor of Keap1 is distinct from those used for electrophilic inducers. Keap1 exploits Cys226, Cys613, and Cys622/624 residues for sensing H_2O_2, and these residues set up an elaborate fail-safe mechanism.

Suzuki et al., 2019, Cell Reports *28*, 746–758
July 16, 2019
https://doi.org/10.1016/j.celrep.2019.06.047

CellPress

OPEN ACCESS
CellPress

Cell Reports
Article

Molecular Mechanism of Cellular Oxidative Stress Sensing by Keap1

Takafumi Suzuki,[1,*] Aki Muramatsu,[1] Ryota Saito,[1] Tatsuro Iso,[1] Takahiro Shibata,[2] Keiko Kuwata,[3] Shin-ichi Kawaguchi,[4] Takao Iwawaki,[5] Saki Adachi,[1] Hiromi Suda,[1] Masanobu Morita,[1] Koji Uchida,[6] Liam Baird,[1] and Masayuki Yamamoto[1,7,8,*]

[1]Department of Medical Biochemistry, Tohoku University Graduate School of Medicine, 2-1 Seiryo-machi, Aoba-ku, Sendai 980-8575, Japan
[2]Graduate School of Bioagricultural Sciences, Nagoya University, Furo-cho, Chikusa, Nagoya 464-8601, Japan
[3]Institute of Transformative Bio-Molecules (WPI-ITbM), Nagoya University, Furo-cho, Chikusa, Nagoya 464-8601, Japan
[4]Center for Education and Research in Agricultural Innovation, Faculty of Agriculture, Saga University, 152-1 Shonan-cho, Karatsu, Saga 847-0021, Japan
[5]Division of Cell Medicine, Department of Life Science, Medical Research Institute, Kanazawa Medical University, 1-1 Daigaku, Uchinada, Kahoku, Ishikawa 920-0293, Japan
[6]Graduate School of Agricultural and Life Sciences, The University of Tokyo, Yayoi 1-1-1, Bunkyo, Tokyo 113-8657, Japan
[7]Tohoku Medical Megabank Organization, Tohoku University, 2-1 Seiryo-machi, Aoba-ku, Sendai 980-8573, Japan
[8]Lead Contact
*Correspondence: taka23@med.tohoku.ac.jp (T.S.), masiyamamoto@med.tohoku.ac.jp (M.Y.)
https://doi.org/10.1016/j.celrep.2019.06.047

SUMMARY

The Keap1-Nrf2 system plays a central role in the oxidative stress response; however, the identity of the reactive oxygen species sensor within Keap1 remains poorly understood. Here, we show that a Keap1 mutant lacking 11 cysteine residues retains the ability to target Nrf2 for degradation, but it is unable to respond to cysteine-reactive Nrf2 inducers. Of the 11 mutated cysteine residues, we find that 4 (Cys226/613/622/624) are important for sensing hydrogen peroxide. Our analyses of multiple mutant mice lines, complemented by MEFs expressing a series of Keap1 mutants, reveal that Keap1 uses the cysteine residues redundantly to set up an elaborate fail-safe mechanism in which specific combinations of these four cysteine residues can form a disulfide bond to sense hydrogen peroxide. This sensing mechanism is distinct from that used for electrophilic Nrf2 inducers, demonstrating that Keap1 is equipped with multiple cysteine-based sensors to detect various endogenous and exogenous stresses.

INTRODUCTION

Oxidative stress is involved in the development and progression of many diseases, including Alzheimer disease, atherosclerosis, and cancer (Finkel and Holbrook, 2000). To overcome this physiological stress, cells are equipped with elaborate defense systems that allow them to maintain homeostasis in an ever-changing environment. The transcription factor Nrf2 (NF-E2-related factor 2) plays a central role in the inducible cytoprotective response to oxidative insults (Itoh et al., 1997; Yamamoto et al., 2018). Under basal unstressed conditions, the Nrf2 protein level is maintained relatively low, due to constitutive ubiquitination mediated by Keap1 (Kelch-like ECH-associated protein 1), an adaptor component of a Cul3 (Cullin 3)-based ubiquitin E3 ligase complex, which targets Nrf2 for proteasomal degradation (Itoh et al., 1999; Kobayashi et al., 2004). Upon exposure to reactive oxygen species (ROS) and electrophiles, the ubiquitination of Nrf2 is repressed, which leads to the stabilization, nuclear translocation, and accumulation of Nrf2, followed by the upregulation of antioxidant gene expression (Ishii et al., 2000; Suzuki et al., 2013).

A multitude of Nrf2 inducers have been reported, most of which are electrophilic and readily react with cysteine thiol groups in Keap1 (Dinkova-Kostova et al., 2002). Keap1 is a cysteine-rich protein possessing 27 and 25 cysteine residues in human and mouse proteins, respectively. A number of *in vitro* labeling and mass spectrometry studies have detected covalent modifications of some of the cysteine residues upon exposure of Keap1 to electrophiles (Dinkova-Kostova et al., 2002; Hong et al., 2005; Eggler et al., 2005; Kobayashi et al., 2009; Hu et al., 2011). The functional significance of these cysteine residues has been examined in experimental systems exploiting site-directed mutagenesis of Keap1 by using reporter co-transfection assays, ectopic overexpression in zebrafish embryos, and transgenic complementation expression in mice (Zhang and Hannink, 2003; Wakabayashi et al., 2004; Eggler et al., 2009; Yamamoto et al., 2008; Kobayashi et al., 2009; Takaya et al., 2012).

We previously generated a Keap1 knockout line of mice and found that the mice are juvenile lethal because of hyperkeratosis in the esophagus and forestomach (Wakabayashi et al., 2003). Of note, this lethality can be rescued by the simultaneous knockout of the *Nrf2* gene, indicating that Nrf2 overexpression causes the phenotype. Mice can also be rescued from the lethality by the concomitant transgenic expression of wild-type Keap1 (Yamamoto et al., 2008). By exploiting this

transgenic complementation rescue analysis technique, we have examined the functions of the sensor cysteine residues of Keap1 in mice *in vivo* (Yamamoto et al., 2008; Takaya et al., 2012). One limitation of this analysis is that the substitution mutations of the cysteine residues should maintain the ubiquitin ligase activity of the Keap1 complex; otherwise, the substitution mutant lines of mice accumulate large amounts of Nrf2, as is the case for Keap1 knockout mice, and therefore sensor function cannot be assessed (Yamamoto et al., 2008; Takaya et al., 2012; Saito et al., 2015).

The functional significance of these cysteine residues culminated in the production of mutant mice with which we conclusively demonstrated that Cys151/Cys273/Cys288 play a fundamental role in the sensing of electrophilic Nrf2-inducing chemicals (Saito et al., 2015). Based on the functional necessity of these three cysteine residues, chemical inducers of Nrf2 were categorized into the following five classes: class I, exemplified by sulforaphane (SFN), dimethyl-fumarate (DMF), and 1-[2-cyano-3,12-dioxooleana-1,9(11)-dien-28-oyl] imidazole (CDDO-Im), all of which are Cys151-dependent compounds; class II, including 15-deoxy-$\Delta^{12,14}$-prostaglandin J_2 (15d-PGJ_2), which uses Cys288; class III, consisting of 4-hydroxy-nonenal (4-HNE), sodium meta-arsenite ($NaAsO_2$), and 9-nitro-octadec-9-enoic acid (9-OA-NO_2), all of which can react with any of the three sensor cysteines Cys151/Cys273/Cys288; class IV, including hydrogen peroxide (H_2O_2), cadmium chloride ($CdCl_2$), zinc chloride ($ZnCl_2$), dexamethasone 21-mesylate (Dex-Mes), and prostaglandin A_2 (PGA_2), all of which activate Nrf2 signaling independently of Cys151/Cys273/Cys288; and class V, consisting of other types of inducers such as Keap1-Nrf2 protein-protein interaction inhibitors (Suzuki and Yamamoto, 2017). The inducers belonging to classes IV and V activate Nrf2 signaling independently of Cys151/Cys273/Cys288.

H_2O_2 plays an important role in cellular physiology and is a key ROS molecule in the development of multiple human diseases (Finkel and Holbrook, 2000). While Nrf2 is often referred to as the "master regulator of the oxidative stress response," the molecular identity of the H_2O_2 sensor in the Keap1-Nrf2 system is unknown. Due to the central role that the Keap1-Nrf2 pathway plays in the oxidative stress response, a thorough and comprehensive understanding of the mechanism by which Keap1 senses and responds to H_2O_2 is required.

In this study, to determine the molecular identity of the H_2O_2 sensor of Keap1, we generated a mouse Keap1 mutant that lacks 11 cysteine residues, making it unable to respond to most cysteine-reactive Nrf2 inducers, including H_2O_2, while retaining the ability to target Nrf2 for ubiquitination and proteasome-dependent degradation. Of the 11 cysteine residues, we found that 4 (Cys226, Cys613, Cys622, and Cys624) are required for H_2O_2-induced Nrf2 activation. Our analyses of mouse embryonic fibroblasts (MEFs) expressing a series of Keap1 mutants, verified by five distinct mutant mouse lines, revealed that Keap1 uses these cysteine residues redundantly to realize a fail-safe mechanism that enables any combination among Cys226, Cys613, and Cys622/624 to form a disulfide bond for sensing hydrogen peroxide.

RESULTS

Generation of 11 Cysteine-less Keap1 Mutant

To provide an insight into the molecular identity of the H_2O_2 sensor of Keap1, we prepared recombinant mouse Keap1 protein and used mass spectrometry to examine the reactivity profile of the cysteine residues of Keap1 with H_2O_2 (Figure S1). Free thiol levels of most cysteine residues in Keap1 were decreased by the addition of 100 μM H_2O_2 (Figure S1A). While no sulfinic and/or sulfonic acids (-SO_2H/-SO_3H) were detected, most of the cysteine residues formed disulfide bonds with small amounts of sulfenic acids (-SOH) (Figures S1B and S1C). These results indicate that *in vitro*, H_2O_2 can oxidize cysteine residues in Keap1 in a non-specific manner, and that the major oxidation product of the cysteine residues of Keap1 is disulfide bond formation. They also suggest that the use of a more physiologically relevant *in vivo* system would provide a better model in which to study the response of Keap1 to H_2O_2.

To fully determine the identity of the H_2O_2 sensor of Keap1, we took the approach of generating a mutant version of Keap1 that could still target Nrf2 for ubiquitin-mediated degradation, but was unable to respond to any cysteine-based Nrf2 inducers, including H_2O_2. To achieve this aim, we generated a number of domain-specific multiple cysteine substitution mutants to determine which combinations of mutations, if any, generate non-functional Keap1 proteins, so that these combinations could be avoided in the subsequent round of mutant Keap1 screening. Thus, the following mutants were generated and screened for their ability to repress Nrf2-dependent gene expression: NTR C-less (C23S&C38S), broad-complex, Tramtrack and Bric-a-Brac (BTB) C-less (C77S&C151S&C171S), intervening region 1 (IVR1) C-less (C196S&C226S&C241S), IVR2 C-less (C249S&C257S&C273W&C288E&C297S), double glycine repeat 1 (DGR1) C-less (C319S&C368S&C395S&C406S&C434S), DGR2 C-less (C489S&C513S&C518S&C583S), and C-terminal region (CTR) C-less (C613S&C622S&C624S) (Figures S2A and S2B). Reporter co-transfection transactivation assays showed that, in contrast to $Keap1^{WT}$, all of the mutants except CTR C-less failed to repress Nrf2 activity. These results imply that these particular combinations of cysteine residue mutations, except those in the CTR domain, affect the ability of Keap1 to ubiquitinate and repress Nrf2 activity, and therefore should be avoided to satisfy our aim of generating a Keap1 mutant that can both target Nrf2 for ubiquitination and not be inactivated by cysteine-based Nrf2 inducers.

Informed by these results, coupled with the knowledge gained from previous studies into the cysteine residues within Keap1 that are modified by electrophilic Nrf2 inducers (Table S1), we introduced mutations into 11 different cysteine residues out of a total of 25 cysteine residues within a single mouse Keap1 protein: Cys151, Cys226, Cys257, Cys273, Cys288, Cys319, Cys434, Cys489, Cys613, Cys622, and Cys624 (Figure 1A). Of note, Cys273 and Cys288 were substituted to tryptophan and glutamic acid, respectively, as the other substitutions were found to abrogate the ubiquitin ligase activity of Keap1 (Saito et al., 2015). The rest of the 11 Cys residues were substituted to serine. We examined whether this $Keap1^{11Cys\text{-}less}$ mutant retains the ability to repress Nrf2 activity

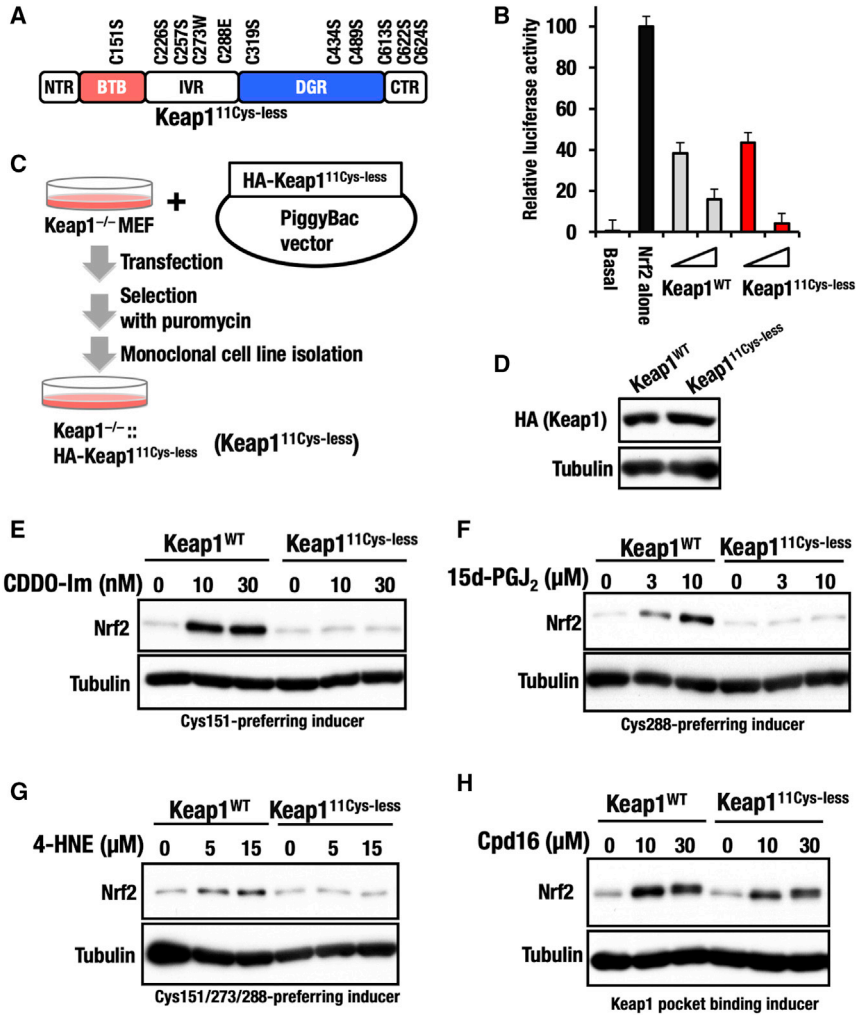

Figure 1. 11-Cys-less Keap1 Mutant

(A) Schematic structure of Keap1$^{11Cys\text{-}less}$ mutant. Keap1 domains; NTR (N-terminal region), BTB (broad-complex, Tramtrack, and Bric-a-Brac), IVR (intervening region), DGR (double glycine repeat), and CTR (C-terminal region).

(B) HEK293T cells were co-transfected with antioxidant response element (ARE)-luciferase reporter vector, Nrf2-overexpressing vector, and vector expressing 8- or 40 ng of Keap1 WT or mutants. Relative luciferase activity was measured 24 h after transfection. Note that Keap1$^{11Cys\text{-}less}$ retains Nrf2 ubiquitination ability comparable to that of wild-type Keap1, so that Nrf2 does not accumulate in Keap1$^{11Cys\text{-}less}$ complemented cells. Data are expressed as means ± SEs; n = 3.

(C) Scheme for complementation of Keap1 in Keap1$^{-/-}$ MEFs. PiggyBac vector expressing HA-tagged Keap1$^{11Cys\text{-}less}$ cDNA and transposase expression vector were co-transfected to Keap1$^{-/-}$ MEFs. Subsequently, several lines of Keap1$^{-/-}$::HA-Keap1$^{11Cys\text{-}less}$ MEFs (Keap1$^{11Cys\text{-}less}$) were established by cloning from single colonies that survived after culture with puromycin.

(D) Western blot analysis of Keap1 expression in Keap1^{WT} and Keap1$^{11Cys\text{-}less}$ MEFs.

(E–H) Keap1^{WT} and Keap1$^{11Cys\text{-}less}$ MEFs treated with 10 or 30 nM CDDO-Im (E), 3 or 10 μM 15d-PGJ_2 (F), 5 or 15 μM 4-HNE (G), or 10 or 30 μM Cpd16 (H) for 3 h were examined by western blotting.

in a reporter co-transfection assay. The Keap1$^{11Cys\text{-}less}$ mutant was able to repress Nrf2 activity in a dose-dependent manner and with a comparable efficiency to Keap1^{WT} (Figure 1B), indicating that the Keap1$^{11Cys\text{-}less}$ mutant retains the ability to repress Nrf2 transcriptional activity.

The Keap1$^{11Cys\text{-}less}$ Mutant Is Insensitive to Most Electrophilic Nrf2 Inducers

Capitalizing on this Keap1$^{11Cys\text{-}less}$ mutant, we addressed the importance of the mutated cysteine residues for the function of Keap1 as a stress sensor. To develop a stable system for the detailed evaluation of the sensor function of Keap1, we generated stable cell lines expressing HA-Keap1$^{11Cys\text{-}less}$ using the PiggyBac transposon system, as described previously (Saito et al., 2015). Expression plasmids for HA-Keap1$^{11Cys\text{-}less}$ were transfected into *Keap1* null MEF cells to rescue the lack of Keap1, and several HA-Keap1$^{11Cys\text{-}less}$ expressing lines were established from single-cell colonies after treatment with puromycin (Figure 1C). Expression levels of the Keap1$^{11Cys\text{-}less}$ protein within the cell lines were evaluated by western blot (Figure 1D), and the lines with comparable expression levels of the Keap1$^{11Cys\text{-}less}$ relative to Keap1^{WT} control were used for further analysis. Consistent with the transient transfection experiments, Keap1$^{11Cys\text{-}less}$ reproducibly repressed basal Nrf2 accumulation in the complemented MEFs (Figures 1E–1H).

We then tested the importance of the 11 mutated cysteine residues for the Keap1-dependent stress response. We challenged the Keap1$^{11Cys\text{-}less}$ MEFs with 30 and 100 μM diethyl maleate (DEM) and 10 and 30 nM CDDO-Im (Keap1-Cys151-preferring Nrf2-inducers), 3 and 10 μM 15d-PGJ_2 (Keap1-Cys288-preferring Nrf2-inducers), 5 and 15 μM 4-HNE, and 3 and 10 μM $NaAsO_2$ (Keap1-Cys151/273/288-selective Nrf2-inducers) (Saito et al., 2015). Consistent with our expectations, Nrf2 accumulation in response to these chemicals was markedly decreased in MEFs expressing Keap1$^{11Cys\text{-}less}$ compared with MEFs expressing Keap1^{WT} (Figures 1E–1G and S2C–S2E), indicating that the Keap1$^{11Cys\text{-}less}$ mutant is unable to respond to these Cys151/273/288-preferring inducers. We also challenged the Keap1$^{11Cys\text{-}less}$ MEFs with 10 and 30 μM compound 16 (Cpd16), a non-electrophilic Nrf2-inducing chemical, which functions as a competitive protein-protein interaction inhibitor of Nrf2 and Keap1 binding (Marcotte et al., 2013). Unlike electrophilic compounds, Nrf2 accumulation upon treatment with Cpd16 was comparable between MEFs expressing Keap1$^{11Cys\text{-}less}$ and Keap1^{WT} (Figure 1H), indicating that the Keap1$^{11Cys\text{-}less}$ mutant responds normally to non-electrophilic inducers.

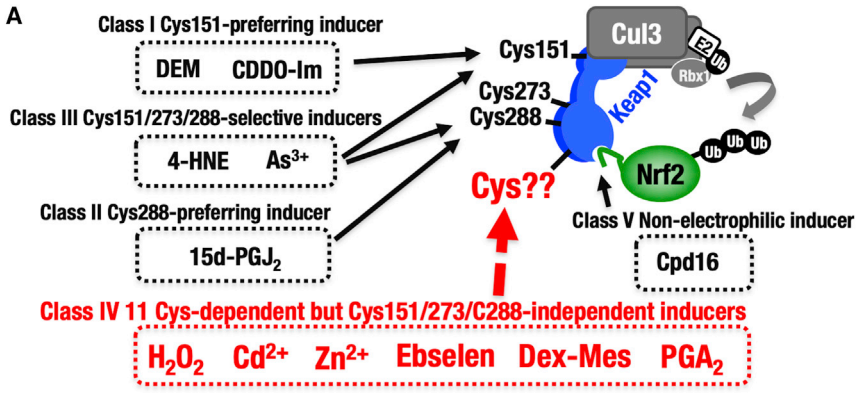

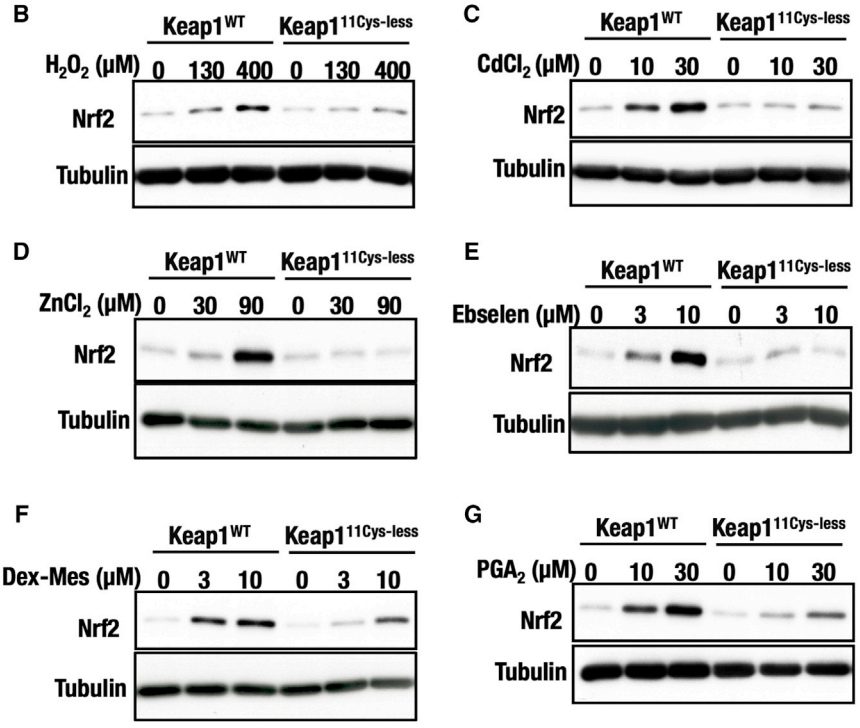

Figure 2. The 11 Cysteine Residues in Keap1 Contain Oxidative Stress Sensors

(A) A classification of Nrf2 inducers based on a previous study that examined the reactivity of Keap1 mutants with the triple sensor-cysteine mutations (i.e., Cys151, Cys273, and Cys288) against various chemical Nrf2 inducers.

(B–G) Keap1^{WT} and Keap1$^{11Cys\text{-}less}$ MEFs treated with 130 or 400 μM H_2O_2 (B), 10 or 30 μM $CdCl_2$ (C), 30 or 90 μM $ZnCl_2$ (D), 3 or 10 μM ebselen (E), 3 or 10 μM Dex-Mes (F), or 10 or 30 μM PGA_2 (G) for 3 h were examined by western blotting.

Sensor or Sensors for Unclassified Nrf2 Inducers Reside within the 11 Cysteine Residues

We next addressed the question of whether the Keap1$^{11Cys\text{-}less}$ mutant is able to respond to unclassified Nrf2-inducing chemicals (Saito et al., 2015)—Cys151/273/288-independent inducers such as hydrogen peroxide (H_2O_2), cadmium chloride ($CdCl_2$), zinc chloride ($ZnCl_2$), ebselen, dexamethasone 21-mesylate (Dex-Mes), and prostaglandin A_2 (PGA_2) (shown in red in Figure 2A). To this end, we challenged the Keap1$^{11Cys\text{-}less}$ MEFs with the above-listed Cys151/273/288-independent inducers and found that in response to all of the Cys151/273/288-independent inducers, Nrf2 accumulation was significantly reduced in MEFs expressing Keap1$^{11Cys\text{-}less}$ (Figures 2B–2G). Thus, our results unequivocally demonstrate that the sensors for these Cys151/273/288-independent inducers reside within the 11 cysteine residues that are mutated in Keap1$^{11Cys\text{-}less}$.

As the Keap1$^{11Cys\text{-}less}$ mutant is unable to sense H_2O_2, we decided to use it as a model in which to examine which cysteine residue or residues are responsible for sensing H_2O_2. Under normal conditions, the sensing of H_2O_2 results in the inactivation of Keap1, meaning that H_2O_2-modified Keap1 is no longer able to function as an E3-ubiquitin ligase for Nrf2. This leads to the accumulation of Nrf2 within the cell, which can be measured by western blot. The genetic inactivation of the H_2O_2 sensor would allow Keap1 to continue to suppress Nrf2 activity, even in cells subject to oxidative stress. Previous experiments using overexpression of transfected Keap1 revealed that H_2O_2 treatment results in disulfide bond formation between Cys226 and Cys613 (Fourquet et al., 2010), suggesting that this cysteine pair may form the H_2O_2 sensor within Keap1 (Hourihan et al., 2013). As Cys226 and Cys613 are both mutated in the Keap1$^{11Cys\text{-}less}$ mutant, we first examined whether Keap1^{C226S} and Keap1^{C613S} are able to respond to H_2O_2 using our complemented MEF approach. In contrast with the previous report, Nrf2 accumulation in response to H_2O_2 in MEFs expressing endogenous levels of Keap1^{C226S} or Keap1^{C613S} was comparable to that of Keap1^{WT} MEFs (Figures S3A–S3C).

We also challenged the MEFs with $CdCl_2$, which along with H_2O_2 belongs to the class of Cys151/273/288-independent inducers (Saito et al., 2015). Similar to H_2O_2, Nrf2 accumulation upon cadmium treatment was comparable to WT in MEFs expressing Keap1^{C226S} or Keap1^{C613S} (Figures S3D and S3E). These observations demonstrate that the disulfide bond formation between Cys226 and Cys613 is dispensable for the sensing of H_2O_2 and cadmium by Keap1, indicating the need to explore a different mechanism through which Keap1 senses H_2O_2 and cadmium to activate Nrf2. Since the substitutions of the 11 cysteine residues substantially abrogated the response, we surmised that the sensor should reside within the 11 cysteine residues.

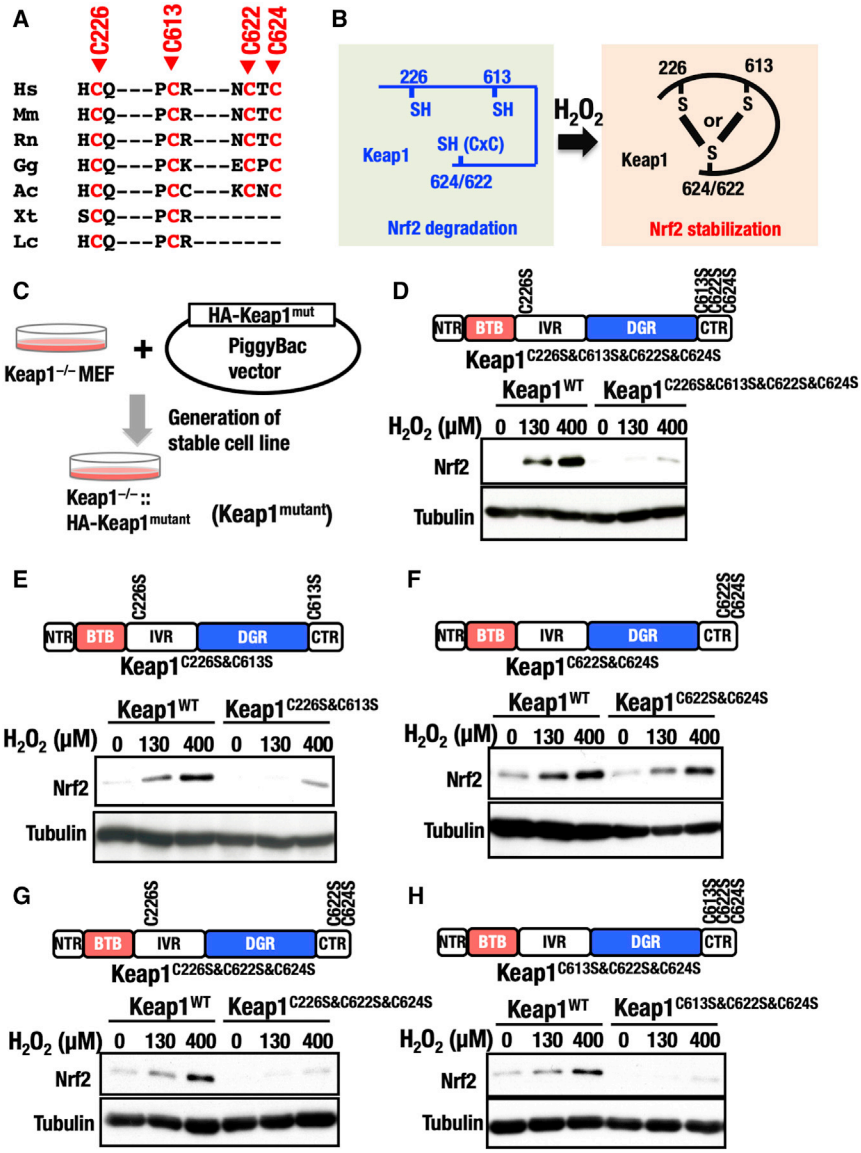

Figure 3. Four Cysteine Residues—Cys226, Cys613, Cys622, and Cys624—Are Important for Sensing Hydrogen Peroxide

(A) A comparison of four cysteine residues (Cys226, Cys613, Cys622, and Cys624) (red) of Keap1 proteins from human (*Hs, Homo sapiens*), mouse (Mm, *Mus musculus*), rat (Rn, *Rattus norvegicus*), chicken (Gg, *Gallus gallus domesticus*), anole lizard (Ac, *Anolis carolinensis*), clawed frog (Xt, *Xenopus tropicalis*), and coelacanth (Lc, *Latimeria chalumnae*).

(B) Hypothetical model that the H_2O_2 sensor in Keap1 may consist of more than two cysteine residues that can form a disulfide bond.

(C) Scheme for complementation of Keap1 in Keap1$^{-/-}$ MEFs. PiggyBac vector expressing hemagglutinin (HA)-tagged Keap1^{mutant} cDNA and transposase expression vector were co-transfected into Keap1$^{-/-}$ MEFs. Subsequently several lines of Keap1$^{-/-}$::HA-Keap1^{mutant} MEFs (Keap1^{mutant}) were established by cloning from single colonies that survived after culture with puromycin.

(D) Keap1^{WT} and Keap1$^{C226S\&C613S\&C622S\&C624S}$ MEFs treated with 130 or 400 μM H_2O_2 for 3 h were examined by western blotting.

(E) Keap1^{WT} and Keap1$^{C226S\&C613S}$ MEFs treated with 130 or 400 μM H_2O_2 for 3 h were examined by western blotting.

(F) Keap1^{WT} and Keap1$^{C622S\&C624S}$ MEFs treated with 130 or 400 μM H_2O_2 for 3 h were examined by western blotting.

(G) Keap1^{WT} and Keap1$^{C226S\&C622S\&C6224S}$ MEFs treated with 130 or 400 μM H_2O_2 for 3 h were examined by western blotting.

(H) Keap1^{WT} and Keap1$^{C613S\&C622S\&C624S}$ MEFs treated with 130 or 400 μM H_2O_2 for 3 h were examined by western blotting.

Cys226, Cys613, and Cys622/Cys624 Are Critical Sensors for H_2O_2

Based on the data obtained so far, we hypothesized that the H_2O_2 sensor in Keap1 may consist of more than two cysteine residues that can form a single disulfide bond. Cognizant of this idea, we considered the H_2O_2-sensing mechanisms of other redox-sensitive proteins and noticed that metallothionein contains a redox active coordination environment consisting of four cysteine residues (Krezel and Maret, 2007). In this configuration, a C-X-C motif within metallothionein is important for cadmium binding (Klassen et al., 2004). As a Cys622-Thr623-Cys624 sequence is found at the C terminus of mammalian Keap1 (Figures 3A and 3B), we decided to examine the contribution of Cys622 and Cys624 for the Keap1-dependent sensing of H_2O_2. Therefore, we introduced mutations into Cys622 and Cys624 of Keap1 and combined the substitution mutations with Cys226 and Cys613 (i.e., Keap1$^{C226S\&C613S\&C622S\&C624S}$). When we examined the response of this quadruple mutant Keap1 to H_2O_2, we found that Nrf2 accumulation in response to H_2O_2 was significantly diminished in MEFs expressing Keap1$^{C226S\&C613S\&C622S\&C624S}$. This observation unequivocally demonstrates that these four cysteine residues (Cys226, Cys613, and Cys622/Cys624) are critical for sensing H_2O_2 (Figures 3C and 3D).

To gain a deeper mechanistic understanding as to how these four cysteine residues function as the H_2O_2 sensor, we generated an additional series of Keap1 mutants. The simultaneous mutation of Cys226 and Cys613 in Keap1$^{C226S\&C613S}$ MEFs resulted in a markedly diminished accumulation of Nrf2 in response to H_2O_2, showing that the sensor is inactive (Figure 3E). In contrast, when Cys622 and Cys624 were simultaneously mutated, Nrf2 accumulation in response to H_2O_2 in the Keap1$^{C622S\&C624S}$ MEFs was comparable to that of the Keap1^{WT} MEFs, suggesting that in this mutant Keap1, the H_2O_2 sensor is still active (Figure 3F). However, the addition of a further mutation to either Cys226 (i.e., Keap1$^{C226S\&C622S\&C624S}$) or Cys613 (i.e., Keap1$^{C613S\&C622S\&C624S}$) inactivated the Keap1 H_2O_2 sensor (Figures 3G and 3H). Taken together with the earlier

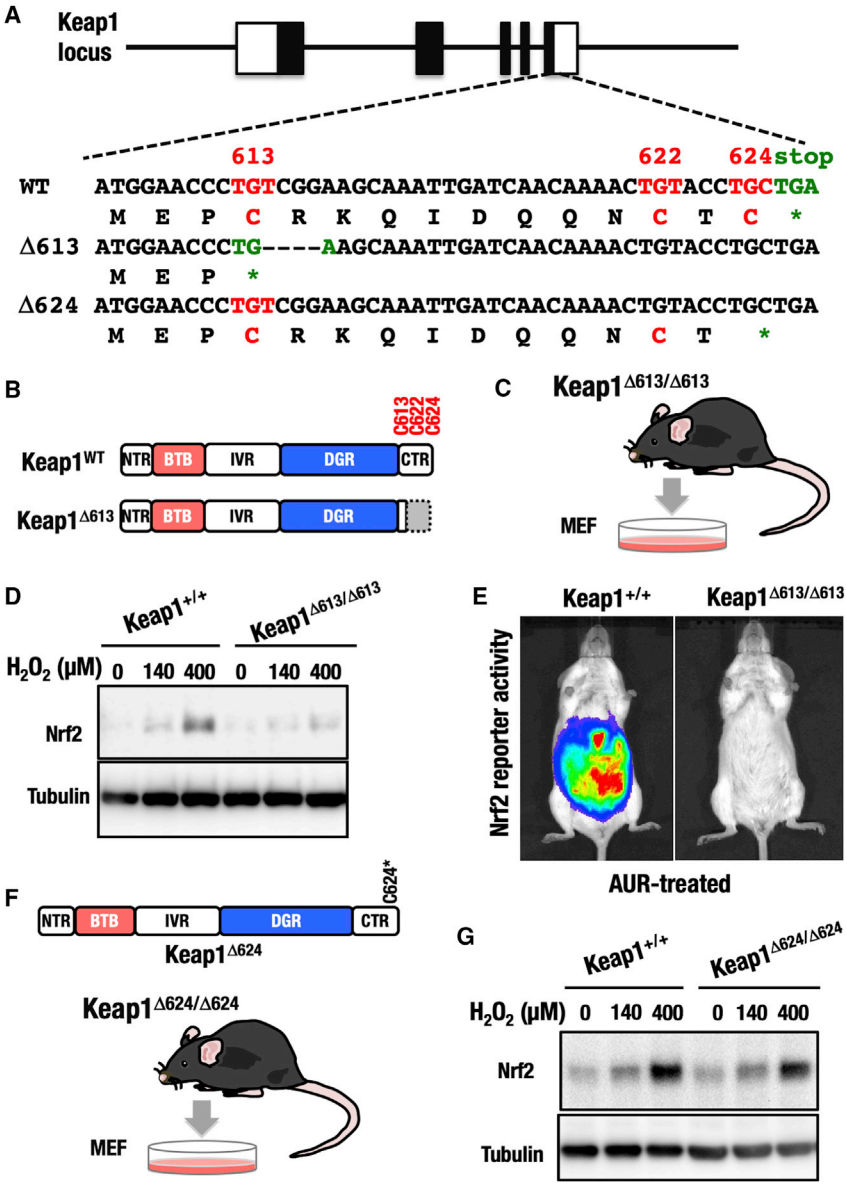

Figure 4. Keap1-CTR Is Required for Sensing Hydrogen Peroxide *In Vivo*

(A) Generation of Keap1$^{\Delta 613}$ or Keap1$^{\Delta 624}$ mice. For the generation of the Keap1$^{\Delta 613}$ mutation, Cys613 was replaced with a stop codon by deleting 4 bp. For the generation of the Keap1$^{\Delta 624}$ mutation, Cys624 was replaced by a stop codon by deleting 3 bp.

(B) Schematic structure of Keap1$^{\Delta 613}$, which lacks region 613–624, including Cys613, Cys622, and Cys624.

(C) Experimental schema for the preparation of MEFs from Keap1$^{\Delta 613/\Delta 613}$ mice.

(D) Keap1$^{+/+}$ and Keap1$^{\Delta 613/\Delta 613}$ MEFs treated with 130 or 400 μM H_2O_2 for 3 h were examined by western blotting.

(E) Representative image of *in vivo* imaging of AUR-induced Nrf2 reporter activity using OKD48::Keap1$^{+/+}$ and OKD48::Keap1$^{\Delta 613/\Delta 613}$ mice. Mice were intraperitoneally injected with 10 mg/kg AUR and subjected to *In Vivo* Imaging System (IVIS) analysis 4 h after AUR administration.

(F) Schematic structure of Keap1$^{\Delta 624}$ and experimental schema for the preparation of MEFs from Keap1$^{\Delta 624/\Delta 624}$ mice.

(G) Keap1$^{+/+}$ and Keap1$^{\Delta 624/\Delta 624}$ MEFs treated with 130 or 400 μM H_2O_2 for 3 h were examined by western blotting.

genome editing. To determine the importance of the three cysteine residues (Cys613, Cys622, and Cys624) in the Keap1-CTR domain, we inserted a stop codon into Cys613 to delete the C terminus of Keap1 (Keap1$^{\Delta 613}$; amino acids 613–624) (Figure 4A); the deletion mutant Keap1$^{\Delta 613}$ lacks the sensor cysteine residues Cys613 and Cys622/Cys624 (Figure 4B). In contrast to the straightforward *Keap1* gene knockout mice that die 3 weeks after birth (Wakabayashi et al., 2003), the Keap1$^{\Delta 613/\Delta 613}$ mice exhibited normal growth and appearance, indicating that Keap1$^{\Delta 613}$ maintains the ability to repress Nrf2 accumulation *in vivo* (Figure S5A).

Cys226 and Cys613 single mutant data, these results revealed that of the three constituent parts of the sensor (Cys226, Cys613, and Cys622/624), any single part is dispensable for the sensing of H_2O_2 by Keap1.

Furthermore, Nrf2 accumulation in response to cadmium in MEFs expressing the same series of Keap1 mutants was largely consistent with the H_2O_2 data (Figure S4), indicating that H_2O_2 and cadmium are commonly sensed by the Cys226, Cys613, and Cys622/Cys624 residues in Keap1.

In Vivo Validation of H_2O_2 Sensors in the Keap1-CTR Domain

To verify the *in vivo* contribution of the herein identified H_2O_2 sensors in Keap1, we generated five lines of mice expressing cysteine mutant versions of Keap1 using CRISPR-mediated

We prepared MEFs from the mice (Figure 4C) and conducted an immunoblot analysis. Results revealed that the basal Nrf2 protein level was suppressed in the Keap1$^{\Delta 613/\Delta 613}$ MEFs at a level comparable to Keap1$^{+/+}$, indicating that Keap1$^{\Delta 613}$ retains the ability to target Nrf2 for ubiquitin-mediated degradation (Figure S5B). To address the question of whether the three C-terminal cysteine residues are required for H_2O_2-mediated activation of Nrf2 signaling, wild-type and Keap1$^{\Delta 613/\Delta 613}$ MEFs were challenged with H_2O_2. We found that Nrf2 accumulation induced by H_2O_2 treatment was significantly diminished in the Keap1$^{\Delta 613/\Delta 613}$ MEFs (Figure 4D). Consistent with this result, NQO1 induction by H_2O_2 was also markedly decreased in the Keap1$^{\Delta 613/\Delta 613}$ MEFs (Figure S5C). We also induced Nrf2 accumulation by glucose oxidase (GO), a continuous generator of H_2O_2, and found that the accumulation was markedly reduced

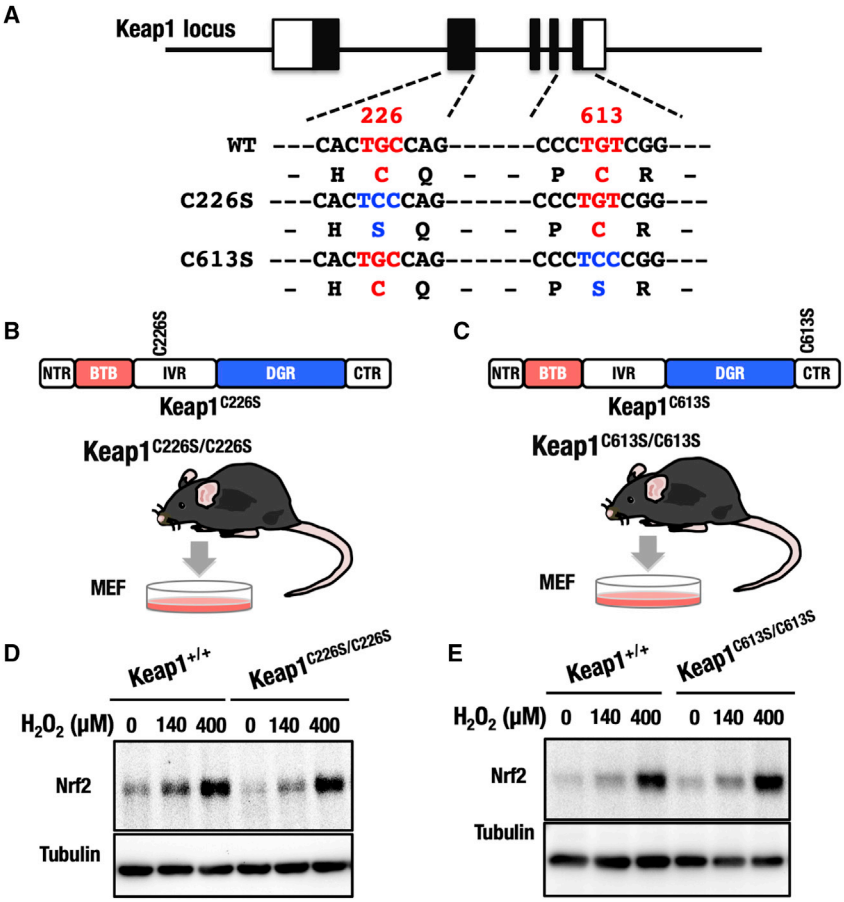

Figure 5. Single Mutations in Cys226 or Cys613 of Keap1 Are Dispensable for H_2O_2 Sensing *In Vivo*

(A) Generation of Keap1^{C226S} and Keap1^{C613S} mice. For the generation of the Keap1^{C226S} mutation, TGC for Cys226 was substituted with TCC for serine. For the generation of the Keap1^{C613S} allele, TGT for Cys613 was substituted with TCC for serine.

(B and C) Schematic structure of Keap1^{C226S} (B) and Keap1^{C613S} (C), and experimental schema for the preparation of MEFs from Keap1$^{C226S/C226S}$ (B) and Keap1$^{C613S/C613S}$ (C) mice.

(D) Keap1$^{+/+}$ and Keap1$^{C226S/C226S}$ MEFs treated with 130 or 400 μM H_2O_2 for 3 h were examined by western blotting.

(E) Keap1$^{+/+}$ and Keap1$^{C613S/C613S}$ MEFs treated with 130 or 400 μM H_2O_2 for 3 h were examined by western blotting.

in the Keap1$^{\Delta613/\Delta613}$ MEFs (Figure S5D). In addition, Nrf2 accumulation induced by the thioredoxin reductase inhibitor auranofin (AUR), which causes an increase in intracellular H_2O_2 levels (Gromer et al., 1998; Marzano et al., 2007), was also diminished in the Keap1$^{\Delta613/\Delta613}$ MEFs (Figure S5E). These results support the notion that these cysteine residues in the CTR function as part of the sensor for H_2O_2.

Nrf2 accumulation in response to DEM (Cys151-preferring inducer) or 15d-PGJ$_2$ (Cys288-preferring inducer) (Figure 2A; Saito et al., 2015) was comparable between Keap1$^{\Delta613/\Delta613}$ and Keap1$^{+/+}$ (Figures S5F and S5G), indicating that Cys613, Cys622, and Cys624 are dispensable for sensing DEM and 15d-PGJ$_2$. These results therefore demonstrate that the mechanism used to sense H_2O_2 is distinct from that used to sense electrophiles.

To further verify this notion *in vivo*, the Nrf2 activity monitoring mouse OKD48 (Oikawa et al., 2012) and the compound OKD48::Keap1$^{\Delta613/\Delta613}$ mice were challenged with the intracellular H_2O_2-inducing compound AUR. While AUR-induced Nrf2 reporter activity was observed in OKD48::Keap1$^{+/+}$ mice, the induction of Nrf2 reporter activity in response to AUR was significantly diminished in OKD48::Keap1$^{\Delta613/\Delta613}$ mice (Figures 4E and S5H), providing further evidence that Cys613 and Cys622/Cys624 are essential for Nrf2 accumulation in response to oxidative stress *in vivo*. These results indicate that these CTR cysteine residues act as sensors of H_2O_2 and are important for Nrf2 accumulation in response to oxidative stress.

Single Mutation in Cys624 of Keap1 Is Dispensable for H_2O_2 Sensing *In Vivo*

To evaluate the effects of a single mutation in Cys624 *in vivo*, we generated mice expressing Keap1$^{\Delta624}$ (Figures 4A and 4F). Keap1$^{\Delta624/\Delta624}$ mice exhibited normal appearance and growth, indicating that Keap1$^{\Delta624}$ maintains the ability to repress Nrf2 accumulation *in vivo*. We prepared MEFs from mice expressing Keap1$^{\Delta624/\Delta624}$ (Figure 4F) and challenged the MEFs with H_2O_2. Consistent with the results of the Keap1-complemented experiments using Keap1 null MEFs (Figure 3), we found that Nrf2 accumulation in MEFs expressing Keap1$^{\Delta624/\Delta624}$ in response to H_2O_2 was comparable to that of Keap1^{WT} MEFs (Figure 4G). In accordance with this result, Nrf2 accumulation induced by the H_2O_2 generator GO was also comparable between Keap1$^{\Delta624/\Delta624}$ and Keap1$^{+/+}$ MEFs (Figure S6B). In addition, AUR-induced Nrf2 accumulation was also commensurate between Keap1$^{\Delta624/\Delta624}$ and Keap1$^{+/+}$ MEFs (Figure S6C). Thus, a single mutation in Cys624 of Keap1 is dispensable for the accumulation of Nrf2 in response to oxidative stress *in vivo*, suggesting that in response to H_2O_2, disulfide bond formation between Cys226 and Cys613 alone is sufficient to abrogate the ubiquitin ligase activity of Keap1.

Single Mutation in Cys226 or Cys613 of Keap1 Is Dispensable for H_2O_2 Sensing *In Vivo*

To clearly determine the importance of Cys226 and Cys613 *in vivo* for the Keap1-dependent H_2O_2 response, we generated mice expressing cysteine to serine mutant versions of Cys226 and Cys613 using CRISPR-mediated genome editing (Figure 5A). Homozygous Keap1$^{C226S/C226S}$ and Keap1$^{C613S/C613S}$ mice exhibited normal appearance and growth, indicating that Keap1^{C226S} and Keap1^{C613S} maintain the ability to repress Nrf2 accumulation *in vivo*. We then prepared MEFs from mice

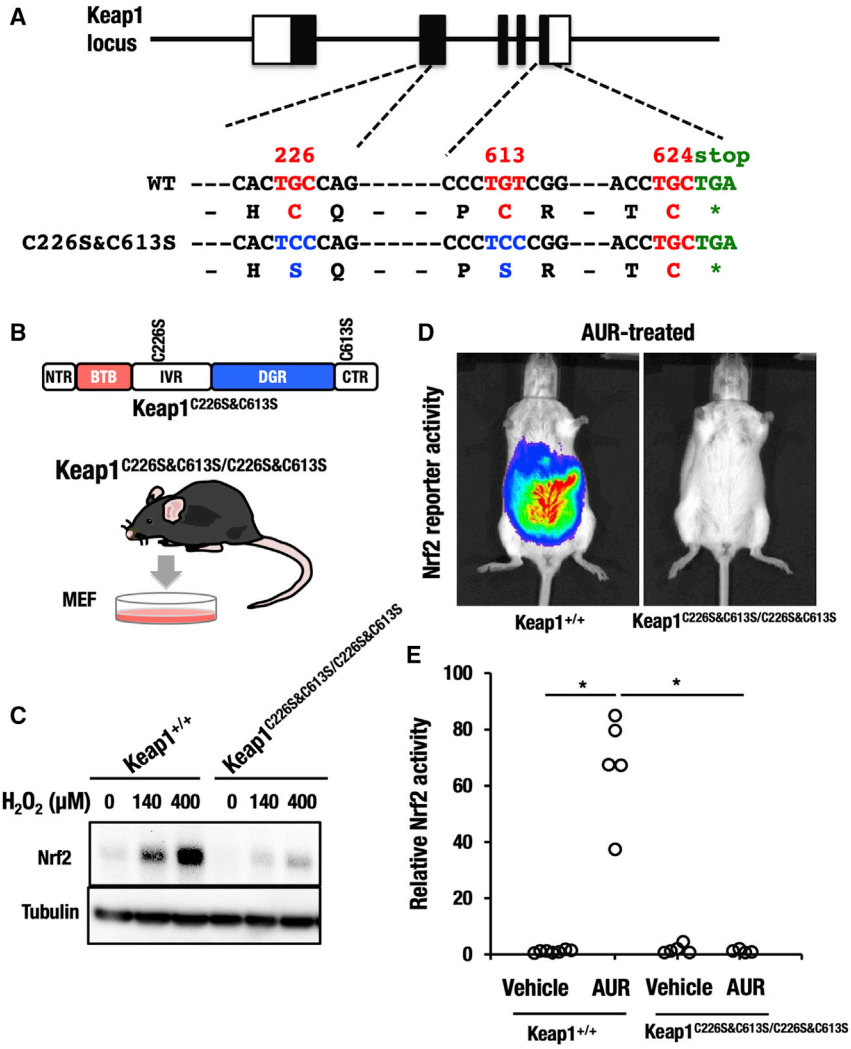

Figure 6. Cys226 and Cys613 Together Are Essential for Sensing Hydrogen Peroxide *In Vivo*

(A) Generation of Keap1$^{C226S\&C613S}$ mice. The Keap1$^{C226S\&C613S}$ mutant was generated by introducing the C226S mutation into the C613S allele.

(B) Schematic structure of Keap1$^{C226S\&C613S}$ and experimental schema for the preparation of MEFs from Keap1$^{C226S\&C613S/C226S\&C613S}$ mice.

(C) Keap1$^{+/+}$ and Keap1$^{C226S\&C613S/C226S\&C613S}$ MEFs treated with 130 or 400 μM H_2O_2 for 3 h were examined by western blotting. Note that this result indicates that a disulfide bond between Cys622 and Cys624 is not sufficient to form a sensor for H_2O_2.

(D) Representative image of *in vivo* imaging of AUR-induced Nrf2 reporter activity using OKD48::Keap1$^{+/+}$ and OKD48::Keap1$^{C226S\&C613S/C226S\&C613S}$ mice. Mice were intraperitoneally injected with 10 mg/kg AUR and subjected to IVIS analysis 4 h after AUR administration.

(E) Relative Nrf2 reporter activity of OKD48::Keap1$^{+/+}$ and OKD48::Keap1$^{C226S\&C613S/C226S\&C613S}$ mice treated with AUR. Statistically significant differences are indicated by asterisks as *p < 0.05; n = 4–7 per genotype.

expressing Keap1$^{C226S/C226S}$ or Keap1$^{C613S/C613S}$ (Figures 5B and 5C) and challenged the MEFs with H_2O_2.

Of note, we found in this study that Nrf2 accumulation in response to H_2O_2 in MEFs expressing endogenous levels of single Cys226 or Cys613 mutant (Keap1^{C226S} or Keap1^{C613S}) was comparable to that of Keap1^{WT} MEFs (Figures 5D and 5E). This is in contrast to the observation in a previous report in which a single Cys226 or Cys613 mutation gives rise to the loss of Nrf2 induction by H_2O_2 (Hourihan et al., 2013). We surmise that in the previous study, high-level overexpression experiments *in transfecto* may have been misleading due to the fact that loading controls and expression levels of the transfected Keap1 mutant proteins relative to untransfected controls were not shown (Hourihan et al., 2013). This may make the data difficult to interpret, as the expression levels of Keap1 mutant proteins fluctuate significantly and endogenous Keap1 seems to interfere with the activity of transfected Keap1. Therefore, mechanistic studies solely based on the Cys226 and Cys613 single mutants would not be able to identify the elaborate H_2O_2 sensor machinery that we have delineated in this study. Our results using stable cell lines and mice support the notion that Cys226, Cys613, and Cys622/Cys624 form an elaborate fail-safe mechanism in which all of the cysteine residues contribute to the H_2O_2 sensor of Keap1, but no single residue is essential for the accumulation of Nrf2 in response to oxidative stress *in vivo*.

The Combination of Cys226 and Cys613 Is Essential for H_2O_2 Sensing *In Vivo*

To assess the contribution of the C226S and C613S double mutation *in vivo*, we generated a mouse line expressing Keap1$^{C226S\&C613S}$ (Figures 6A and 6B). The Keap1-C226S mutation was introduced into Keap1$^{C613S/+}$ fertilized eggs using CRISPR-Cas9 genome editing, and mating the founder mice with wild-type mice resulted in the generation of Keap1$^{C226S\&C613S/+}$ mice. Homozygous mice (Keap1$^{C226S\&C613S/C226S\&C613S}$) exhibited normal growth and appearance (Figure S7A), indicating that Keap1$^{C226S\&C613S}$ maintains the ability to repress Nrf2 accumulation *in vivo*. We prepared MEFs from Keap1$^{C226S\&C613S/C226S\&C613S}$ mice (Figure 6C). Immunoblot analysis revealed that the basal Nrf2 protein level was suppressed in the Keap1$^{C226S\&C613S/C226S\&C613S}$ MEFs at a level comparable to Keap1$^{+/+}$, indicating that Keap1$^{C226S\&C613S}$ retains the ability to target Nrf2 for ubiquitin-mediated degradation (Figure S7B). Nrf2 accumulation in response to DEM (Cys151-preferring inducer) or 15d-PGJ$_2$ (Cys288-preferring inducer) (Saito et al., 2015) was also comparable between Keap1$^{C226S\&C613S/C226S\&C613S}$ and Keap1$^{+/+}$ (Figures S7C and S7D), indicating that Cys226 and Cys613 are dispensable for sensing DEM and 15d-PGJ$_2$.

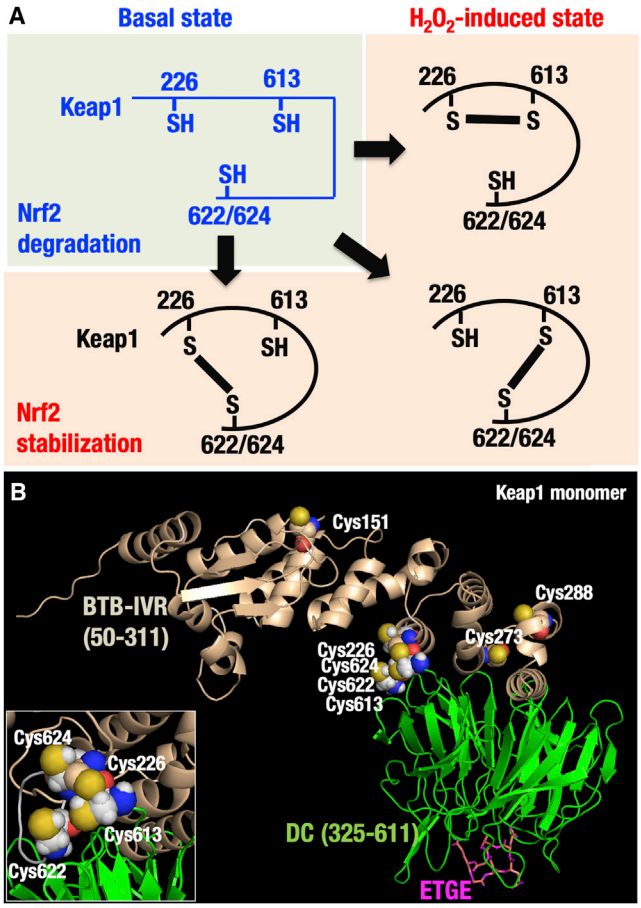

Figure 7. A Model for the Oxidative Stress Sensor in Keap1

(A) Hypothetical model of disulfide bond formation among Cys226, Cys613, and Cys622/624 in Keap1 in response to oxidative stress. This is a mechanism for the oxidative stress response by the Keap1-Nrf2 system in which H_2O_2 induces the formation of a disulfide bond between any combination of two from three parts of the sensor (Cys226, Cys613, and Cys622/624), which causes a conformational change in Keap1, resulting in Keap1 inactivation and Nrf2 stabilization.

(B) A structure model of a Keap1 monomer generated based on information about the Keap1 DC domain (amino acids 325–611) and the BTB-IVR region of KLHL11. Insets show a cluster of Cys226, Cys613, Cys622, and Cys624. Green, beige, and magenta domains indicate Keap1-DC, BTB-IVR, and the ETGE motif of Nrf2, respectively. Yellow, red, and blue atoms indicate sulfur, oxygen, and nitrogen, respectively.

Nrf2 accumulation induced by the H_2O_2 generator GO was markedly diminished in Keap1$^{C226S\&C613S/C226S\&C613S}$ MEFs (Figure S7E), while AUR-induced Nrf2 accumulation was significantly reduced in Keap1$^{C226S\&C613S/C226S\&C613S}$ MEFs (Figure S7F). The induction of Nrf2 reporter activity in response to AUR was also significantly diminished in OKD48::Keap1$^{C226S\&C613S/C226S\&C613S}$ mice (Figures 6D and 6E), providing further evidence that the Cys226 and Cys613 combination is essential for Nrf2 accumulation in response to oxidative stress *in vivo*.

Thus, Keap1 is equipped with an H_2O_2 sensor that comprises three distinct parts: Cys226, Cys613, and Cys622/624. As any single mutation in one of the three parts does not give rise to the loss-of-sensor-function or the accumulation of Nrf2 in response to H_2O_2, we surmise that any combination of two of these cysteine residues is essential for the sensor function of Keap1 for H_2O_2. Therefore, we propose an elaborate fail-safe mechanism using these cysteine residues for sensing oxidative stresses.

DISCUSSION

Whereas Keap1 is a well-established regulator of the cellular response to oxidative stress, the exact mechanism through which it senses this stress remains unknown. To identify the oxidative stress sensor within Keap1, in this study we generated a Keap1 mutant in which 11 cysteine residues are substituted to other amino acid residues (Keap1$^{11Cys\text{-}less}$ mutant), including all of the major sensor cysteine residues, Cys151, Cys273, and Cys288. We found that the Keap1$^{11Cys\text{-}less}$ mutant cell line failed to respond to H_2O_2, indicating that the sensor(s) for H_2O_2 exists within the 11 substituted cysteine residues. Further analyses using mutant cell lines revealed that four cysteine residues, Cys226, Cys613, Cys622, and Cys624, form the H_2O_2 sensor of Keap1. To verify the H_2O_2 sensor within Keap1, we generated multiple mutant mouse lines. Analyses of these mice revealed that four cysteine residues make up the Keap1 H_2O_2 sensor. As summarized in Figure 7A, our analyses of the MEFs and mice revealed that Keap1 uses the cysteine residues to set up an elaborate fail-safe mechanism enabling any combination among Cys226, Cys613, and Cys622/Cys624 to form a disulfide bond for the sensing of H_2O_2. This sensing mechanism is distinct from that used by electrophilic Nrf2 inducers. Thus, Keap1 is equipped with multiple cysteine residues that act specifically and/or collaboratively as sensors for the detection of a wide range of endogenous and exogenous stresses.

The majority of activators of the Keap1-Nrf2 pathway are classified as electrophiles, which react with single cysteine residues in Keap1 by forming a C-S bond with the cysteine thiol group. For example, Cys151 of Keap1 is responsible for sensing the electrophile DEM (Takaya et al., 2012; Saito et al., 2015). In contrast, ROS such as H_2O_2 usually form intra- or inter-molecular disulfide bonds between two cysteine residues (Okazaki et al., 2007). Although we cannot fully refute the possibility that H_2O_2 signaling is mediated indirectly by thiol redox mediators, we found that disulfide bond formation in Keap1 was induced by H_2O_2. This fact suggests that the mechanism through which H_2O_2 inactivates Keap1 may be direct and distinct from that used by typical Nrf2-inducing electrophiles.

It has previously been proposed that the ability of Keap1 to sense H_2O_2 is dependent on the formation of a disulfide bond between Cys226 and Cys613, which induces a conformational change in Keap1 (Fourquet et al., 2010; Hourihan et al., 2013). In addition, a single mutation in either Cys226 and Cys613 has been shown to inhibit the ability of Keap1 to sense and respond to H_2O_2 and cadmium (McMahon et al., 2010; Hourihan et al., 2013). However, our experimental approach using stable cell lines and mice do not support these findings. We found that even when Cys226 or Cys613 are individually mutated, Keap1 retains the ability to respond to H_2O_2 and cadmium, indicating

that the formation of a disulfide bond between Cys226 and Cys613 cannot explain the mechanism through which Keap1 senses H_2O_2. In a previous report, the H_2O_2-induced band shift of Keap1 in a reduced gel was canceled by the mutation either of Cys226 or Cys613 (Fourquet et al., 2010); however, our results imply that this band shift does not reflect the inactivation of Keap1 by oxidation.

Informed by these results, we hypothesized that the Keap1 H_2O_2 sensor may consist of additional cysteine residues that function together with Cys226 and Cys613 to sense oxidative stress. To address this hypothesis, we generated a Keap1 mutant protein with 11 cysteine residue substitutions, along with various individual point mutants and combinations of multiple mutations, to the cysteine residues. Functional analyses of this range of Keap1 mutants showed that the H_2O_2 sensor resides in the 11 cysteine residues and finally revealed that Cys622 and Cys624 are also involved in the sensing of H_2O_2 by Keap1. Despite the fact that our results delineate that the four cysteine residues are involved in the H_2O_2 sensor activity, no individual cysteine residue is critical for the sensor function, as the single mutation of any of the four cysteine residues does not inactivate the oxidative stress sensor. These observations support our contention that the sensor for the physiological stressor H_2O_2 contains a robust compensatory mechanism. Thus, we found that an elaborate fail-safe mechanism consisting of Cys226, Cys613, and Cys622/Cys624 ensures that Keap1 is able to respond to H_2O_2 across a range of conditions.

To determine whether there is a hierarchy within the four residues of the H_2O_2 sensor, we simultaneously mutated multiple cysteine residues within a single Keap1 protein. We found that any single mutation to any one of the three parts of the sensor is dispensable for its function. This leads to a model in which any combination of two of the three parts of the sensor are able to form a disulfide bond (Cys226-Cys613, Cys226-Cys622/624, or Cys613-Cys622/624) to function as an H_2O_2 sensor. This fail-safe mechanism enables the remaining cysteine residues to rescue the H_2O_2 sensor function in the absence of any single part (Figure 7A). The mechanism provides a significant advantage to cells, because if some of the cysteine residues become unreactive due to oxidation to sulfinic and/or sulfonic acids or due to alkylation, this fail-safe mechanism could ensure that Keap1 is still responsive to H_2O_2. Cys226 and Cys613 are highly conserved from fish to mammals, while Cys622 and Cys624 are found only in mammals, birds, and reptiles (Figure 3A; Fuse and Kobayashi, 2017), suggesting that Cys226 and Cys613 were acquired early in evolution as the main sensor, while Cys622 and Cys624 were acquired later, potentially allowing terrestrial animals to adapt to a hyperoxic environment during the evolution from water- to land-based habitats.

Disulfide bond formation between Cys226, Cys613, and Cys622/624 in response to oxidative stress suggests that these four cysteine residues may be located in close proximity and form a redox-active cluster. A Keap1 structural model generated based on information from the Keap1 DC domain (amino acids 325–611) (Padmanabhan et al., 2006) and KLHL11 (Canning et al., 2013) suggests that Cys226 in the IVR resides in the vicinity of the CTR, including Cys613, Cys622, and Cys624 (Figure 7B). In addition, the IVR domain was found to surround the DGR domain in our electron microscope analysis (Ogura et al., 2010), and therefore the proximity between the IVR and DGR domains supports the notion that Cys226 and Cys613/622/624 are clustered together. An example of an analogous structure to the one proposed is provided by metallothionein, which binds zinc through clusters of thiolate bonds (Klassen et al., 2004; Krezel and Maret, 2007). Keap1 has previously been reported to be a zinc-thiol protein (Dinkova-Kostova et al., 2005), and therefore the four cysteine residues that make up the H_2O_2 sensor in Keap1 may form a similar redox active coordination environment to metallothionein.

Our experimental approach revealed that the Nrf2-inducing activity of cadmium works through a mechanism similar to that for H_2O_2. It has been shown that the effect of cadmium on Nrf2 accumulation is abolished by the addition of the antioxidant *N*-acetyl cysteine (NAC) (Lee et al., 2011), suggesting that the four cysteine residues of Keap1 identified in this study may sense cellular H_2O_2 generated as a second messenger by cadmium treatment.

In this study, we found that AUR activates Nrf2 via the same oxidative stress sensor of Keap1 as H_2O_2 and cadmium. AUR is a drug approved for the treatment of rheumatoid arthritis, but it is also being investigated for potential therapeutic applications in a number of diseases, including cancer, neurodegenerative disorders, and bacterial infection (Roder and Thomson, 2015). Although the pharmacological mechanism of action has not been fully elucidated, an Nrf2-inducing activity of AUR has been reported (Kataoka et al., 2001), which may explain its anti-inflammatory properties. As AUR is an established thioredoxin reductase inhibitor (Gromer et al., 1998), the four cysteine residues identified in this study may sense cellular H_2O_2 derived by the inhibition of thioredoxin reductase, or they may normally be maintained in a reduced form via the thioredoxin system. Therefore, this study provides valuable information regarding the Nrf2 activation mechanism by AUR in light of recent drug-repositioning efforts.

In conclusion, in this study we have answered the long-standing question of how our body senses and adapts to oxidative stress. Identification of the sensor cysteine residues revealed that Keap1 directly senses oxidative stress through an elaborate fail-safe mechanism and that this sensing mechanism is distinct from that of electrophilic Nrf2 inducers. Our present findings also provide insights into the multiple sensing mechanisms used to detect various environmental stimuli *in vivo*.

STAR★METHODS

Detailed methods are provided in the online version of this paper and include the following:

- KEY RESOURCES TABLE
- LEAD CONTACT AND MATERIALS AVAILABILITY
- EXPERIMENTAL MODEL AND SUBJECT DETAILS
  - Establishment of stable cell lines that express transfected Keap1
  - Mice
  - Generation of MEFs from Keap1 mutant knock-in mice

SUPPLEMENTAL INFORMATION

Supplemental Information can be found online at https://doi.org/10.1016/j.celrep.2019.06.047.

ACKNOWLEDGMENTS

This work was supported in part by the Ministry of Education, Culture, Sports, Science and Technology/Japan Society for the Promotion of Science Grants-in-Aid for Scientific Research (MEXT/JSPS KAKENHI) (24249015, 26111002, 19H01019, and 18K19417, to M.Y., and 26460354, 25112502, 19K07340, 18H04963, 17K15590, 17KK0183, and 26111010, to T. Suzuki), Project for Cancer Research and Therapeutic Evolution, Japan Agency for Medical Research and Development (to M.Y.), and Takeda Science Foundation (to M.Y. and T. Suzuki).

We thank Drs. Hozumi Motohashi, Seizo Koshiba, Tsunehiro Mizushima, Fumiki Katsuoka, and Tadayuki Tsujita for discussion and advice. We also thank Mr. Takahiro Yamamoto and the Biomedical Research Core of Tohoku University Graduate School of Medicine for technical support. ITbM is supported by the World Premier International Research Center Initiative, Japan.

AUTHOR CONTRIBUTIONS

T. Suzuki, A.M., R.S., and M.Y. designed the research and analyzed the data. T. Suzuki, A.M., R.S., and T. Iso conducted the experiments. T. Shibata, K.K., and K.U. performed the mass spectrometry analysis. S.K. synthesized the Cpd16 compound. T. Iwawaki provided OKD48 mice. T. Suzuki, S.A., H.S., and M.M. generated the Keap1 mutant mice. T. Suzuki, L.B., and M.Y. wrote the paper.

DECLARATION OF INTERESTS

The authors declare no competing interests.

Received: January 17, 2019
Revised: April 20, 2019
Accepted: June 12, 2019
Published: July 16, 2019

SUPPORTING CITATIONS

The following references appear in the Supplemental Information: Abiko et al. (2011); Adam et al. (2011); Copple et al. (2008); Dietz et al. (2008); Fujii et al. (2010); Holland et al. (2008); Kansanen et al. (2011); Luo et al. (2007); Ooi et al. (2011); Rachakonda et al. (2008); Tsujita et al. (2011); Yoshida et al. (2014).

REFERENCES

Abiko, Y., Miura, T., Phuc, B.H., Shinkai, Y., and Kumagai, Y. (2011). Participation of covalent modification of Keap1 in the activation of Nrf2 by tert-butylbenzoquinone, an electrophilic metabolite of butylated hydroxyanisole. Toxicol. Appl. Pharmacol. *255*, 32–39.

Adam, J., Hatipoglu, E., O'Flaherty, L., Ternette, N., Sahgal, N., Lockstone, H., Baban, D., Nye, E., Stamp, G.W., Wolhuter, K., et al. (2011). Renal cyst formation in Fh1-deficient mice is independent of the Hif/Phd pathway: roles for fumarate in KEAP1 succination and Nrf2 signaling. Cancer Cell *20*, 524–537.

Canning, P., Cooper, C.D., Krojer, T., Murray, J.W., Pike, A.C., Chaikuad, A., Keates, T., Thangaratnarajah, C., Hojzan, V., Ayinampudi, V., et al. (2013). Structural basis for Cul3 protein assembly with the BTB-Kelch family of E3 ubiquitin ligases. J. Biol. Chem. *288*, 7803–7814.

Copple, I.M., Goldring, C.E., Jenkins, R.E., Chia, A.J., Randle, L.E., Hayes, J.D., Kitteringham, N.R., and Park, B.K. (2008). The hepatotoxic metabolite of acetaminophen directly activates the Keap1-Nrf2 cell defense system. Hepatology *48*, 1292–1301.

Dietz, B.M., Liu, D., Hagos, G.K., Yao, P., Schinkovitz, A., Pro, S.M., Deng, S., Farnsworth, N.R., Pauli, G.F., van Breemen, R.B., and Bolton, J.L. (2008). Angelica sinensis and its alkylphthalides induce the detoxification enzyme NAD(P)H: quinone oxidoreductase 1 by alkylating Keap1. Chem. Res. Toxicol. *21*, 1939–1948.

Dinkova-Kostova, A.T., Holtzclaw, W.D., Cole, R.N., Itoh, K., Wakabayashi, N., Katoh, Y., Yamamoto, M., and Talalay, P. (2002). Direct evidence that sulfhydryl groups of Keap1 are the sensors regulating induction of phase 2 enzymes that protect against carcinogens and oxidants. Proc. Natl. Acad. Sci. USA *99*, 11908–11913.

Dinkova-Kostova, A.T., Holtzclaw, W.D., and Wakabayashi, N. (2005). Keap1, the sensor for electrophiles and oxidants that regulates the phase 2 response, is a zinc metalloprotein. Biochemistry *44*, 6889–6899.

Eggler, A.L., Liu, G., Pezzuto, J.M., van Breemen, R.B., and Mesecar, A.D. (2005). Modifying specific cysteines of the electrophile-sensing human Keap1 protein is insufficient to disrupt binding to the Nrf2 domain Neh2. Proc. Natl. Acad. Sci. USA *102*, 10070–10075.

Eggler, A.L., Small, E., Hannink, M., and Mesecar, A.D. (2009). Cul3-mediated Nrf2 ubiquitination and antioxidant response element (ARE) activation are dependent on the partial molar volume at position 151 of Keap1. Biochem. J. *422*, 171–180.

Finkel, T., and Holbrook, N.J. (2000). Oxidants, oxidative stress and the biology of ageing. Nature *408*, 239–247.

Fourquet, S., Guerois, R., Biard, D., and Toledano, M.B. (2010). Activation of NRF2 by nitrosative agents and H2O2 involves KEAP1 disulfide formation. J. Biol. Chem. *285*, 8463–8471.

Fujii, S., Sawa, T., Ihara, H., Tong, K.I., Ida, T., Okamoto, T., Ahtesham, A.K., Ishima, Y., Motohashi, H., Yamamoto, M., and Akaike, T. (2010). The critical role of nitric oxide signaling, via protein S-guanylation and nitrated cyclic GMP, in the antioxidant adaptive response. J. Biol. Chem. *285*, 23970–23984.

Fuse, Y., and Kobayashi, M. (2017). Conservation of the Keap1-Nrf2 System: An Evolutionary Journey through Stressful Space and Time. Molecules *22*, E436.

Gromer, S., Arscott, L.D., Williams, C.H., Jr., Schirmer, R.H., and Becker, K. (1998). Human placenta thioredoxin reductase. Isolation of the selenoenzyme, steady state kinetics, and inhibition by therapeutic gold compounds. J. Biol. Chem. *273*, 20096–20101.

Hayashi, M., Takai, J., Yu, L., Motohashi, H., Moriguchi, T., and Yamamoto, M. (2015). Whole-Body In Vivo Monitoring of Inflammatory Diseases Exploiting Human Interleukin 6-Luciferase Transgenic Mice. Mol. Cell. Biol. *35*, 3590–3601.

Holland, R., Hawkins, A.E., Eggler, A.L., Mesecar, A.D., Fabris, D., and Fishbein, J.C. (2008). Prospective type 1 and type 2 disulfides of Keap1 protein. Chem. Res. Toxicol. *21*, 2051–2060.

Hong, F., Freeman, M.L., and Liebler, D.C. (2005). Identification of sensor cysteines in human Keap1 modified by the cancer chemopreventive agent sulforaphane. Chem. Res. Toxicol. *18*, 1917–1926.

Hourihan, J.M., Kenna, J.G., and Hayes, J.D. (2013). The gasotransmitter hydrogen sulfide induces nrf2-target genes by inactivating the keap1 ubiquitin ligase substrate adaptor through formation of a disulfide bond between cys-226 and cys-613. Antioxid. Redox Signal. *19*, 465–481.

Hu, C., Eggler, A.L., Mesecar, A.D., and van Breemen, R.B. (2011). Modification of keap1 cysteine residues by sulforaphane. Chem. Res. Toxicol. *24*, 515–521.

Ishii, T., Itoh, K., Takahashi, S., Sato, H., Yanagawa, T., Katoh, Y., Bannai, S., and Yamamoto, M. (2000). Transcription factor Nrf2 coordinately regulates a group of oxidative stress-inducible genes in macrophages. J. Biol. Chem. *275*, 16023–16029.

Iso, T., Suzuki, T., Baird, L., and Yamamoto, M. (2016). Absolute Amounts and Status of the Nrf2-Keap1-Cul3 Complex within Cells. Mol. Cell. Biol. *36*, 3100–3112.

Itoh, K., Chiba, T., Takahashi, S., Ishii, T., Igarashi, K., Katoh, Y., Oyake, T., Hayashi, N., Satoh, K., Hatayama, I., et al. (1997). An Nrf2/small Maf heterodimer mediates the induction of phase II detoxifying enzyme genes through antioxidant response elements. Biochem. Biophys. Res. Commun. *236*, 313–322.

Itoh, K., Wakabayashi, N., Katoh, Y., Ishii, T., Igarashi, K., Engel, J.D., and Yamamoto, M. (1999). Keap1 represses nuclear activation of antioxidant responsive elements by Nrf2 through binding to the amino-terminal Neh2 domain. Genes Dev. *13*, 76–86.

Kang, M.I., Kobayashi, A., Wakabayashi, N., Kim, S.G., and Yamamoto, M. (2004). Scaffolding of Keap1 to the actin cytoskeleton controls the function of Nrf2 as key regulator of cytoprotective phase 2 genes. Proc. Natl. Acad. Sci. USA *101*, 2046–2051.

Kansanen, E., Bonacci, G., Schopfer, F.J., Kuosmanen, S.M., Tong, K.I., Leinonen, H., Woodcock, S.R., Yamamoto, M., Carlberg, C., Ylä-Herttuala, S., et al. (2011). Electrophilic nitro-fatty acids activate NRF2 by a KEAP1 cysteine 151-independent mechanism. J. Biol. Chem. *286*, 14019–14027.

Kataoka, K., Handa, H., and Nishizawa, M. (2001). Induction of cellular antioxidative stress genes through heterodimeric transcription factor Nrf2/small Maf by antirheumatic gold(I) compounds. J. Biol. Chem. *276*, 34074–34081.

Klassen, R.B., Crenshaw, K., Kozyraki, R., Verroust, P.J., Tio, L., Atrian, S., Allen, P.L., and Hammond, T.G. (2004). Megalin mediates renal uptake of heavy metal metallothionein complexes. Am. J. Physiol. Renal Physiol. *287*, F393–F403.

Kobayashi, A., Kang, M.I., Okawa, H., Ohtsuji, M., Zenke, Y., Chiba, T., Igarashi, K., and Yamamoto, M. (2004). Oxidative stress sensor Keap1 functions as an adaptor for Cul3-based E3 ligase to regulate proteasomal degradation of Nrf2. Mol. Cell. Biol. *24*, 7130–7139.

Kobayashi, M., Li, L., Iwamoto, N., Nakajima-Takagi, Y., Kaneko, H., Nakayama, Y., Eguchi, M., Wada, Y., Kumagai, Y., and Yamamoto, M. (2009). The antioxidant defense system Keap1-Nrf2 comprises a multiple sensing mechanism for responding to a wide range of chemical compounds. Mol. Cell. Biol. *29*, 493–502.

Krezel, A., and Maret, W. (2007). Different redox states of metallothionein/thionein in biological tissue. Biochem. J. *402*, 551–558.

Lee, Y.J., Lee, G.J., Baek, B.J., Heo, S.H., Won, S.Y., Im, J.H., Cho, M.K., Nam, H.S., and Lee, S.H. (2011). Cadmium-induced up-regulation of aldo-keto reductase 1C3 expression in human nasal septum carcinoma RPMI-2650 cells: involvement of reactive oxygen species and phosphatidylinositol 3-kinase/Akt. Environ. Toxicol. Pharmacol. *31*, 469–478.

Luo, Y., Eggler, A.L., Liu, D., Liu, G., Mesecar, A.D., and van Breemen, R.B. (2007). Sites of alkylation of human Keap1 by natural chemoprevention agents. J. Am. Soc. Mass Spectrom. *18*, 2226–2232.

Marcotte, D., Zeng, W., Hus, J.C., McKenzie, A., Hession, C., Jin, P., Bergeron, C., Lugovskoy, A., Enyedy, I., Cuervo, H., et al. (2013). Small molecules inhibit the interaction of Nrf2 and the Keap1 Kelch domain through a non-covalent mechanism. Bioorg. Med. Chem. *21*, 4011–4019.

Maruyama, A., Tsukamoto, S., Nishikawa, K., Yoshida, A., Harada, N., Motojima, K., Ishii, T., Nakane, A., Yamamoto, M., and Itoh, K. (2008). Nrf2 regulates the alternative first exons of CD36 in macrophages through specific antioxidant response elements. Arch. Biochem. Biophys. *477*, 139–145.

Marzano, C., Gandin, V., Folda, A., Scutari, G., Bindoli, A., and Rigobello, M.P. (2007). Inhibition of thioredoxin reductase by auranofin induces apoptosis in cisplatin-resistant human ovarian cancer cells. Free Radic. Biol. Med. *42*, 872–881.

McMahon, M., Lamont, D.J., Beattie, K.A., and Hayes, J.D. (2010). Keap1 perceives stress via three sensors for the endogenous signaling molecules nitric oxide, zinc, and alkenals. Proc. Natl. Acad. Sci. USA *107*, 18838–18843.

Ogura, T., Tong, K.I., Mio, K., Maruyama, Y., Kurokawa, H., Sato, C., and Yamamoto, M. (2010). Keap1 is a forked-stem dimer structure with two large spheres enclosing the intervening, double glycine repeat, and C-terminal domains. Proc. Natl. Acad. Sci. USA *107*, 2842–2847.

Ohta, T., Iijima, K., Miyamoto, M., Nakahara, I., Tanaka, H., Ohtsuji, M., Suzuki, T., Kobayashi, A., Yokota, J., Sakiyama, T., et al. (2008). Loss of Keap1 function activates Nrf2 and provides advantages for lung cancer cell growth. Cancer Res. *68*, 1303–1309.

Oikawa, D., Akai, R., Tokuda, M., and Iwawaki, T. (2012). A transgenic mouse model for monitoring oxidative stress. Sci. Rep. *2*, 229.

Okazaki, S., Tachibana, T., Naganuma, A., Mano, N., and Kuge, S. (2007). Multistep disulfide bond formation in Yap1 is required for sensing and transduction of H2O2 stress signal. Mol. Cell *27*, 675–688.

Ooi, A., Wong, J.C., Petillo, D., Roossien, D., Perrier-Trudova, V., Whitten, D., Min, B.W., Tan, M.H., Zhang, Z., Yang, X.J., et al. (2011). An antioxidant response phenotype shared between hereditary and sporadic type 2 papillary renal cell carcinoma. Cancer Cell *20*, 511–523.

Padmanabhan, B., Tong, K.I., Ohta, T., Nakamura, Y., Scharlock, M., Ohtsuji, M., Kang, M.I., Kobayashi, A., Yokoyama, S., and Yamamoto, M. (2006). Structural basis for defects of Keap1 activity provoked by its point mutations in lung cancer. Mol. Cell *21*, 689–700.

Rachakonda, G., Xiong, Y., Sekhar, K.R., Stamer, S.L., Liebler, D.C., and Freeman, M.L. (2008). Covalent modification at Cys151 dissociates the electrophile sensor Keap1 from the ubiquitin ligase CUL3. Chem. Res. Toxicol. *21*, 705–710.

Roder, C., and Thomson, M.J. (2015). Auranofin: repurposing an old drug for a golden new age. Drugs R D. *15*, 13–20.

Saito, R., Suzuki, T., Hiramoto, K., Asami, S., Naganuma, E., Suda, H., Iso, T., Yamamoto, H., Morita, M., Baird, L., et al. (2015). Characterizations of Three Major Cysteine Sensors of Keap1 in Stress Response. Mol. Cell. Biol. *36*, 271–284.

Shindo, N., Fuchida, H., Sato, M., Watari, K., Shibata, T., Kuwata, K., Miura, C., Okamoto, K., Hatsuyama, Y., Tokunaga, K., et al. (2019). Selective and reversible modification of kinase cysteines with chlorofluoroacetamides. Nat. Chem. Biol. *15*, 250–258.

Suzuki, T., and Yamamoto, M. (2017). Stress-sensing mechanisms and the physiological roles of the Keap1-Nrf2 system during cellular stress. J. Biol. Chem. *292*, 16817–16824.

Suzuki, T., Kelly, V.P., Motohashi, H., Nakajima, O., Takahashi, S., Nishimura, S., and Yamamoto, M. (2008). Deletion of the selenocysteine tRNA gene in macrophages and liver results in compensatory gene induction of cytoprotective enzymes by Nrf2. J. Biol. Chem. *283*, 2021–2030.

Suzuki, T., Motohashi, H., and Yamamoto, M. (2013). Toward clinical application of the Keap1-Nrf2 pathway. Trends Pharmacol. Sci. *34*, 340–346.

Takaya, K., Suzuki, T., Motohashi, H., Onodera, K., Satomi, S., Kensler, T.W., and Yamamoto, M. (2012). Validation of the multiple sensor mechanism of the Keap1-Nrf2 system. Free Radic. Biol. Med. *53*, 817–827.

Tsujita, T., Li, L., Nakajima, H., Iwamoto, N., Nakajima-Takagi, Y., Ohashi, K., Kawakami, K., Kumagai, Y., Freeman, B.A., Yamamoto, M., and Kobayashi, M. (2011). Nitro-fatty acids and cyclopentenone prostaglandins share strategies to activate the Keap1-Nrf2 system: a study using green fluorescent protein transgenic zebrafish. Genes Cells *16*, 46–57.

Wakabayashi, N., Itoh, K., Wakabayashi, J., Motohashi, H., Noda, S., Takahashi, S., Imakado, S., Kotsuji, T., Otsuka, F., Roop, D.R., et al. (2003). Keap1-null mutation leads to postnatal lethality due to constitutive Nrf2 activation. Nat. Genet. *35*, 238–245.

Wakabayashi, N., Dinkova-Kostova, A.T., Holtzclaw, W.D., Kang, M.I., Kobayashi, A., Yamamoto, M., Kensler, T.W., and Talalay, P. (2004). Protection

against electrophile and oxidant stress by induction of the phase 2 response: fate of cysteines of the Keap1 sensor modified by inducers. Proc. Natl. Acad. Sci. USA *101*, 2040–2045.

Watai, Y., Kobayashi, A., Nagase, H., Mizukami, M., McEvoy, J., Singer, J.D., Itoh, K., and Yamamoto, M. (2007). Subcellular localization and cytoplasmic complex status of endogenous Keap1. Genes Cells *12*, 1163–1178.

Yamamoto, T., Suzuki, T., Kobayashi, A., Wakabayashi, J., Maher, J., Motohashi, H., and Yamamoto, M. (2008). Physiological significance of reactive cysteine residues of Keap1 in determining Nrf2 activity. Mol. Cell. Biol. *28*, 2758–2770.

Yamamoto, M., Kensler, T.W., and Motohashi, H. (2018). The KEAP1-NRF2 System: a Thiol-Based Sensor-Effector Apparatus for Maintaining Redox Homeostasis. Physiol. Rev. *98*, 1169–1203.

Yoshida, E., Abiko, Y., and Kumagai, Y. (2014). Glutathione adduct of methylmercury activates the Keap1-Nrf2 pathway in SH-SY5Y cells. Chem. Res. Toxicol. *27*, 1780–1786.

Zhang, D.D., and Hannink, M. (2003). Distinct cysteine residues in Keap1 are required for Keap1-dependent ubiquitination of Nrf2 and for stabilization of Nrf2 by chemopreventive agents and oxidative stress. Mol. Cell. Biol. *23*, 8137–8151.

STAR★METHODS

KEY RESOURCES TABLE

REAGENT or RESOURCE	SOURCE	IDENTIFIER
Antibodies		
Rat monoclonal anti-Nrf2	Maruyama et al., 2008	RRID:AB_2756449
Rat monoclonal anti-HA	Roche	3F10; RRID:AB_2314622
Rat monoclonal anti-Keap1	Watai et al., 2007	RRID:AB_2756450
Mouse anti-α-Tubulin	Sigma	DM1A; RRID:AB_477593
Bacterial and Virus Strains		
Rosetta 2 (DE3)	Millipore Corporation	Cat#71400
Chemicals, Peptides, and Recombinant Proteins		
Alt-R® S.p. Cas9 Nuclease V3	Integrated DNA Technologies	Cat#1081058
Diethylmaleate	Wako Chemicals	Cat#059-02052
Cadmium chloride	Wako Chemicals	Cat#032-00122
Zinc chloride	Wako Chemicals	Cat#266-00288
Dexamethasone 21-mesylate	Wako Chemicals	Cat#041-18861
Auranofin	Wako Chemicals	Cat#012-25081
Hydrogen peroxide	Wako Chemicals	Cat#088-01187
15-deoxy-delta^{12,14}-prostaglandin J_2	Cayman Chemical	Cat#18570
Prostaglandin A_2	Cayman Chemical	Cat#14010
L-sulforaphane	Sigma Aldrich	Cat#S6317
tert-butyl hydroquinone	Sigma Aldrich	Cat#112941
4-hydroxy-nonenal	Santa Cruz	Cat#sc-202019
CDDO-Im	Mochida Pharmaceuticals Company	N/A
Cpd16	Jiang al, 2014	N/A
Critical Commercial Assays		
Dual-Luciferase reporter system	Promega	https://www.promega.com/resources/protocols/technical-manuals/0/dual-luciferase-reporter-assay-system-protocol/
Sepazol®-RNA I Super G RNA extraction kit	Nacalai	Cat#09379
ReverTra Ace® qPCR RT Master Mix	TOYOBO	Cat#FSG-201
Experimental Models: Cell Lines		
Mouse; Keap1-null MEFs	Ohta et al., 2008	N/A
Human; HEK293T	ATCC	CRL-3216
Experimental Models: Organisms/Strains		
Mouse Slc:BDF1	SLC	N/A
Mouse B6N-Tyr$^{c\text{-}Brd}$/BrdCrCrl	Charles River	N/A
Mouse C57BL/6J-Tg(3xARE/TK-NRF2/luc)M2Tiw (OKD48)	RIKEN BRC	RBRC05704
Oligonucleotides		
See Table S2 for all CRISPR guide sequence	This study	N/A
Targeting oligonucleotide for C226S: GCTTCCCTTCTCA CCTGAGCTCCCTGCAGGTGGCCAAGCAGGAGGAGTT CTTCAACCTGTCACACTCCCAGCTGGCCACGCTCATC AGCCGGGATGATCTGAACGTACGCTGCGAGTCCGAG GTGTTCCACGC	This study	N/A

(*Continued on next page*)

Continued		
REAGENT or RESOURCE	SOURCE	IDENTIFIER
Targeting oligonucleotide for C613S: ATGACATCTGGCC GCAGCGGGGTGGGTGTGGCCGTCACCATGGAACCCT CCCGGAAGCAAATTGATCAACAAAACTCTACCAGCTG AAGCACTTGGTGAAGCACTTGGAATACCTGAGCACTG ACAACAGG	This study	N/A
See Table S3 for all primers used for genotyping	This study	N/A
See Table S3 for primers used for RT-qPCR	Suzuki et al., 2008	N/A
Recombinant DNA		
pColdIII	Takara	Cat#3363
The PiggyBac transposon vector system	System Biosciences	Cat#PB514B-2
pEF-HA-Keap1	Yamamoto et al., 2008	N/A
pNqo1-ARE-Luc	Kang et al., 2004	N/A
pRL-TK	Promega	AF025846
p3xFlag-Nrf2	Kang et al., 2004	N/A
Software and Algorithms		
Living Image software	PerkinElmer	https://www.perkinelmer.com/lab-products-and-services/resources/in-vivo-imaging-software-downloads.html
Proteome Discoverer 2.2.0.388 / SEQUEST	Thermo	https://www.thermofisher.com/order/catalog/product/OPTON-30795
PyMOL	Schrödinger LLC	https://pymol.org/2/
SWISS-MODEL Homology Modeling	Swiss Institute of Bioinformatics	https://swissmodel.expasy.org/
JMP	SAS	https://www.jmp.com/global-geo-redirects/geohome.html

LEAD CONTACT AND MATERIALS AVAILABILITY

Further information and requests for resources and reagents should be directed to and will be fulfilled by the Lead Contact, Masayuki Yamamoto (masiyamamoto@med.tohoku.ac.jp).

EXPERIMENTAL MODEL AND SUBJECT DETAILS

Establishment of stable cell lines that express transfected Keap1

The PiggyBac transposon vector system (PB514B-2, System Biosciences) was used to establish stable cell lines that express HA-tagged Keap1 cDNA. Mouse Keap1 cDNA mutants were inserted into the PiggyBac expression vector as previously described (Saito et al., 2015). Immortalized *Keap1* null MEFs (Wakabayashi et al., 2003; Ohta et al., 2008) were maintained in DMEM (1 mg/ml glucose, Wako Chemical) containing 10% fetal bovine serum (FBS). Co-transfection of the PiggyBac expression vector plus the transposase plasmid was performed by electroporation with double 1100 V pulse for 30 ms. After 2-3 days culture, electroporated cells were selected using 2 μg/ml of puromycin for 7-10 days. Expression of RFP (red fluorescent protein) was verified under a fluorescence microscope, and several individual colonies were selected and grown for further analysis.

Mice

All mice were treated according to the regulations of The Standards for Human Care and Use of Laboratory Animals of Tohoku University (Sendai, Japan) and the Guidelines for Proper Conduct of Animal Experiments of the Ministry of Education, Culture, Sports, Science, and Technology of Japan. All animal experiments were executed with the approval of the Tohoku University Animal Care Committee.

$Keap1^{\Delta 613/\Delta 613}$, $Keap1^{\Delta 624/\Delta 624}$, $Keap1^{C613S/C613S}$, $Keap1^{C226S/C226S}$ or $Keap1^{C226S\&C613S/C226S\&C613S}$ were generated with CRISPR/Cas9-mediated homologous recombination of a single-stranded oligodeoxynucleotide (ssODN) containing the point mutation (Integrated DNA Technologies). Guide RNAs targeting each position surrounding cysteine residues of Keap1 were designed and purchased from FASMAC (GE-003). Cas9 protein (Integrated DNA Technologies, 1081058), guide RNA and the targeting oligonucleotide (Integrated DNA Technologies) were electroporated into fertilized eggs derived from BDF1 parents. Founder mice were

screened by PCR genotyping and confirmed by direct sequencing. Sequence information of the guide RNAs and genotyping primers are shown in Tables S2 and S3. The founder mice were crossed with wild-type mice to ensure that the mutations were transmitted to the germline. Keap1^{C226S} and Keap1$^{C226S\&C613S}$ mice were generated by introducing the C226S mutation into fertilized eggs derived from wild-type and Keap1$^{C613S/C613S}$ mice respectively. By crossing the heterozygous mutants, homozygotes were obtained. The genotyping was done by Taqman real-time PCR (Applied Biosystems). Sequence information of the genotyping primers and probes are shown in Table S3.

The Nrf2 activity monitoring mouse OKD48 (RBRC05704) (Oikawa et al., 2012) was provided by RIKEN BRC which is participating in the National BioResource Project of MEXT/AMED, Japan. Sequence information of primers for PCR genotyping is shown in Table S3. *In vivo* bioluminescence imaging was conducted utilizing an *in vivo* imaging system (IVIS) (PerkinElmer) as previously described (Hayashi et al., 2015). Briefly, mice were crossed with albino C57BL/6 and injected intraperitoneally with 75 mg/kg D-luciferin. Five minutes after the luciferin injection, the mice were anesthetized with isoflurane. Subsequently, the mice were placed in a light-sealed chamber and the luciferase activity was imaged for 1 min. Photons emitted from various regions of the mice were quantified using Living Image software (PerkinElmer). A combination of male and female mice at 6-12 weeks of age were used in the experiments.

Generation of MEFs from Keap1 mutant knock-in mice

MEFs were prepared from individual embryos of Keap1$^{+/+}$, Keap1$^{\Delta613/\Delta613}$, Keap1$^{\Delta624/\Delta624}$, Keap1$^{C613S/C613S}$, Keap1$^{C226S/C226S}$ or Keap1$^{C226S\&C613S/C226S\&C613S}$ at embryonic Day 13.5. Sex of embryos were not determined. The head and internal organs were removed, and the torso was minced and dispersed in 0.25% trypsin-EDTA. After incubation for 24 h, culture medium was exchanged with fresh medium to remove non-adherent cells. Adherent cells were subsequently maintained and passaged. MEFs were maintained in DMEM (1 mg/ml glucose, Wako Chemical) containing 10% fetal bovine serum (FBS).

METHOD DETAILS

Recombinant Keap1 protein

6xHis-tagged mouse Keap1 cDNA was cloned into the pColdIII vector (Takara 3363). 6xHis-tagged protein of Keap1 was expressed in bacteria Rosetta 2 (DE3) (Millipore Corporation 71400) and purified (Iso et al., 2016). The protein was purified using Ni-NTA (QIAGEN 30230) and digested with TurboTEV protease (Nacalai 08461). After removal of His-tag by Ni-NTA, flow-through was purified with MonoQ and Superdex 200 column chromatography (GE Healthcare). The proteins were near homogeneity, as judged by sodium dodecyl sulfate-polyacrylamide gel electrophoresis (SDS-PAGE). The amounts of purified protein were determined by a comparison with a BSA standard.

Transfection experiments and measuring luciferase activity

All amino acid substitutions were introduced by PCR into an EF-1α promoter-driven HA-tagged mouse Keap1 expression vector as previously described (Yamamoto et al., 2008). Transfection experiments were performed using Lipofectamine (Invitrogen) as previously described (Kang et al., 2004). For measuring luciferase activity, HEK293T cells were transfected with 100-ng p*Nqo1*-ARE-Luc plasmid, 10-ng pRL-TK transfection control plasmid (Promega), 8-ng p3xFlag-Nrf2 plasmid (Kang et al., 2004) and 8- or 40-ng wild-type or mutant Keap1 expression plasmids. Luciferase activity was measured using the Dual-Luciferase reporter system (Promega).

RNA extraction and quantitative real-time PCR

Total RNAs were prepared from MEFs using a Sepazol®-RNA I Super G RNA extraction kit (Nacalai). The cDNAs were synthesized from total RNA using ReverTra Ace® qPCR RT Master Mix with gDNA Remover (TOYOBO). Real-time quantitative PCR was performed using QuantStudio (Applied Biosystems). The primer and probe sequences used for detecting *NAD(P)H:quinone oxidoreductase 1* (*NQO1*) have been described previously (Suzuki et al., 2008).

Immunoblotting

Whole cell extracts were prepared in a sample buffer (20% glycerol, 4% SDS, 0.125M Tris-HCl [pH 6.8], and 0.2M dithiothreitol) from MEFs or macrophages treated with Nrf2-inducing chemicals for 3 hours. The protein samples were subjected to 8% SDS-polyacrylamide gel electrophoresis (SDS-PAGE) and electro-transferred to PVDF membranes. Specific protein signals were detected by anti-Nrf2 (Maruyama et al., 2008; 1:200 dilution, RRID:AB_2756449), anti-HA (Roche 3F10; 1:1000 dilution; RRID:AB_2314622), anti-Keap1 (Watai et al., 2007; 1:200 dilution; RRID:AB_2756450) or anti-α-Tubulin (T9026, Sigma DM1A; 1:1000 dilution; RRID:AB_477593) antibodies.

Model building

A structure model of a Keap1 monomer was generated by using SWISS-MODEL Homology Modeling (https://swissmodel.expasy.org/). A figure of the model was prepared using PyMOL.

Mass spectrometry analysis of Keap1 cysteine oxidation

Recombinant mouse Keap1 protein was expressed in bacteria and purified as previously described (Iso et al., 2016). The Keap1 was dissolved in 20-mM Tri-HCl buffer (pH 8.0) containing 100-mM NaCl and 1-mM Tris(2-carboxyethyl)phosphine as stock solution. After buffer exchange to 20-mM Tris-HCl buffer (pH 7.4) containing 100-mM NaCl using MicroSpin G-25 (GE-Healthcare) columns, the Keap1 protein (1 mg/ml) was reacted with H_2O_2 (0-100 μM) for 30 min at 37°C. Following incubation, the samples were treated with dimedone (final 10 mM) and iodoacetamide (final 20 mM) for 30 min at room temperature in the dark. The proteins were precipitated with chloroform/methanol, washed with cold acetone, and redissolved with 4-M urea buffer. The resulting samples were reduced with Tris(2-carboxyethyl)phosphine (final 16.7 mM) for 1 hour and alkylated with *N*-ethylmaleimide (final 25 mM) for 1 hour. The samples were separated by SDS-PAGE and the protein bands corresponding to Keap1 were excised and digested with trypsin. Samples were analyzed by nano-flow reverse phase liquid chromatography followed by tandem MS, using a Q Exactive hybrid mass spectrometer (Thermo) as previously described (Shindo et al., 2019). MS/MS spectra were interpreted and peak lists were generated by Proteome Discoverer 2.2.0.388 (Thermo). Searches were performed by using the SEQUEST (Thermo) against the mouse Keap1 peptide sequence for cysteine modification site identification. Peptide identifications were based on significant Xcorr (high confidence filter). Peptide identification and modification information returned from SEQUEST were manually inspected and filtered to obtain confirmed peptide identification and modification lists of HCD MS/MS.

QUANTIFICATION AND STATISTICAL ANALYSIS

Statistical Analysis

Statistical analyses were performed using JMP Pro. Data are expressed as mean ± SE. The sample size is indicated in the figure legends and represents biological replicate. Statistical significance was evaluated using the two-way ANOVA for two variables. A p value of < 0.05 was considered to be statistically significant.

Cell Reports, Volume *28*

Supplemental Information

Molecular Mechanism of Cellular Oxidative Stress Sensing by Keap1

Takafumi Suzuki, Aki Muramatsu, Ryota Saito, Tatsuro Iso, Takahiro Shibata, Keiko Kuwata, Shin-ichi Kawaguchi, Takao Iwawaki, Saki Adachi, Hiromi Suda, Masanobu Morita, Koji Uchida, Liam Baird, and Masayuki Yamamoto

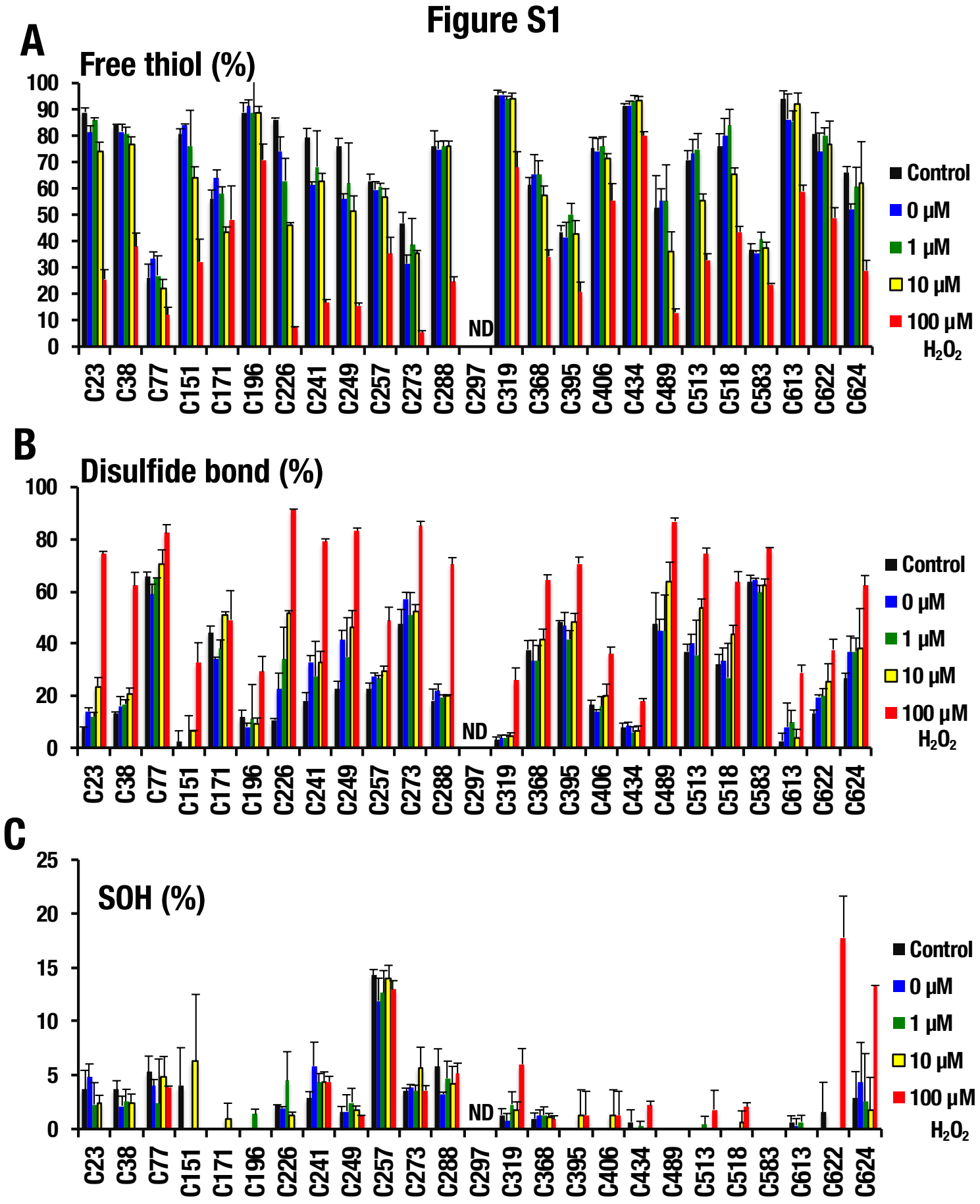

Figure S1. The reactivity profile of Keap1's cysteine residues with H_2O_2 (Related to Figure 1)

(**A**) Percentages of free thiol content of Keap1's cysteine residues.

(**B**) Percentages of disulfide bond formation between Keap1's cysteine residues. (**C**) Percentages of sulfenic acid formation in Keap1's cysteine residues. ND indicates not detected. Data are expressed as mean ± SE (n=3).

Figure S2

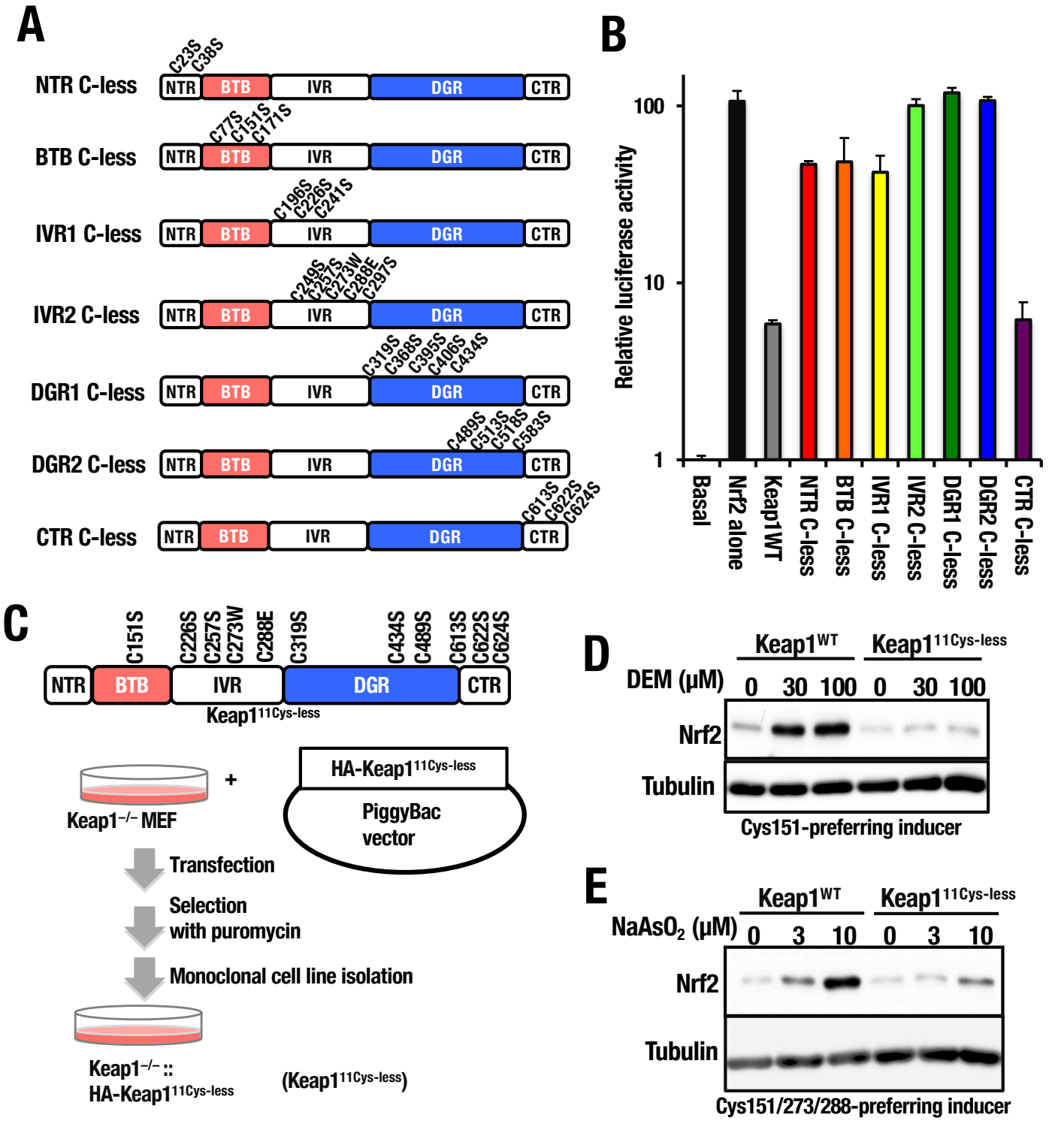

Figure S2. Domain-specific multiple cysteine substitution mutants of Keap1 and Keap1$^{11Cys\text{-}less}$ mutant (Related to Figure 1)

(**A**) Schematic structures of Keap1 mutants lacking cysteine residues in each of the different domains.

(**B**) HEK293T cells were co-transfected with an ARE-luciferase reporter vector, Nrf2-overexpression vector, and a vector expressing Keap1 WT or a member of the Keap1 mutant series. 24 hours after transfection, relative luciferase activity was measured. Keap1 domains: NTR (N-terminal region), BTB (Broad-complex, Tramtrack and Bric-a-Brac), IVR (Intervening region), DGR (Double glycine repeat), and CTR (C-terminal region).

(C) Keap1$^{-/-}$::HA-Keap1$^{11Cys\text{-}less}$ MEFs (Keap1$^{11Cys\text{-}less}$) were established, and used for analysis.

(D and **E)** The ability of WT and mutant Keap1 to repress Nrf2 accumulation in response to inducers was examined by Western blot. Keap1^{WT} and Keap1$^{11Cys\text{-}less}$ MEFs were treated with 30- or 100-μM DEM **(D)**, or 3- or 10-μM $NaAsO_2$ **(E)** for 3 hours.

Figure S3

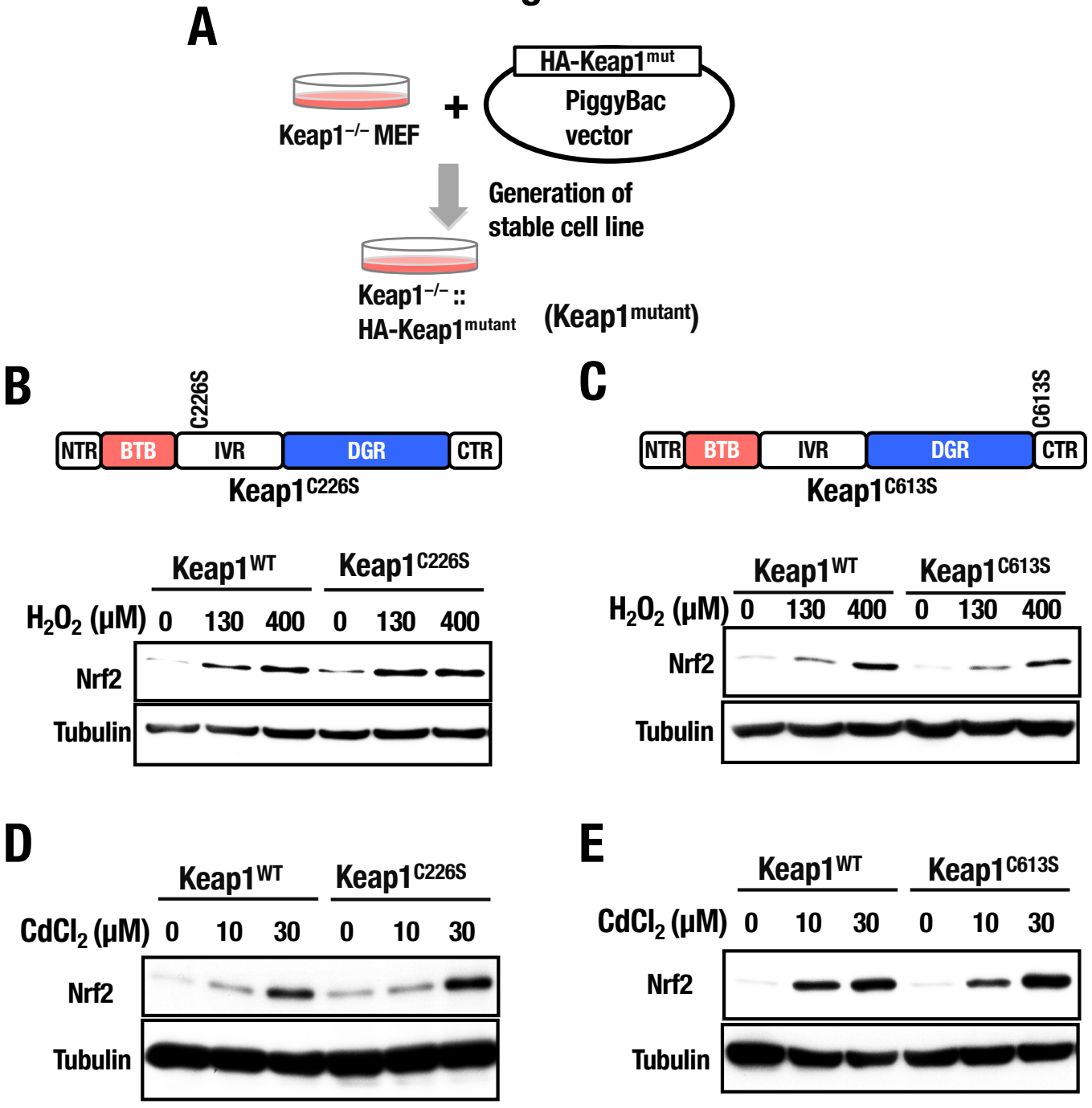

Figure S3. Keap1^{C226S} and Keap1^{C613S} are able to respond to H_2O_2 (Related to Figure 3).
(**A**) Scheme for complementation of Keap1 in Keap1$^{-/-}$ MEFs. A PiggyBac vector expressing HA-tagged Keap1^{mutant} cDNA and transposase expression vector were co-transfected to Keap1$^{-/-}$ MEFs. Subsequently several lines of Keap1$^{-/-}$ ::HA-Keap1^{mutant} MEFs (Keap1^{mutant}) were established by cloning from single-colonies which survived after culture with puromycin. (**B-E**) The ability of WT and mutant Keap1 to repress Nrf2 accumulation in response to inducers was examined by Western blot. Keap1^{WT}, Keap1^{C226S} (**B, D**) and Keap1^{C613S} MEFs (**C, E**) were treated with 130- or 400-μM H_2O_2 (**B, C**) or 10- or 30-μM $CdCl_2$ (**D, E**) for 3 hours.

Figure S4

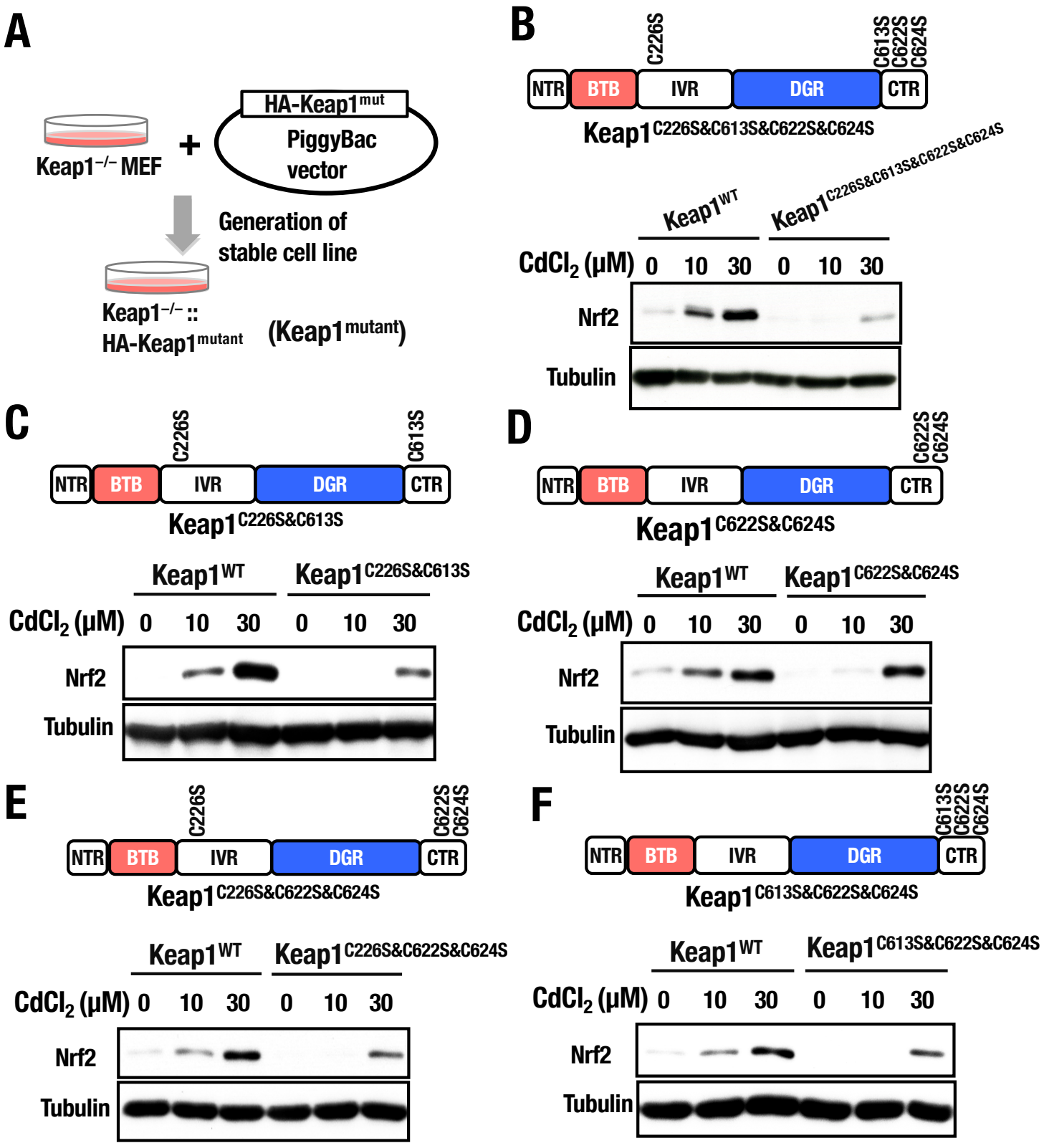

Figure S4. Cadmium is sensed by the Cys226, Cys613, and Cys622/Cys624 residues in Keap1 (Related to Figure 3). (**A**) Scheme for complementation of Keap1 in Keap1$^{-/-}$ MEFs. PiggyBac vector expressing HA-tagged Keap1^{mutant} cDNA and transposase expression vector were co-transfected to Keap1$^{-/-}$ MEFs. Subsequently several lines of Keap1$^{-/-}$::HA-Keap1^{mutant} MEFs (Keap1^{mutant}) were established by cloning from single-colonies which survived after culture with puromycin. (**B-F**) The ability of WT and mutant Keap1 to repress Nrf2 accumulation in response to $CdCl_2$ was examined by Western blot. Keap1^{WT} and Keap1$^{C226S\&C613S\&C622S\&C624S}$ (**B**), Keap1$^{C226S\&C613S}$ (**C**), Keap1$^{C622S\&C624S}$ (**D**), Keap1$^{C226S\&C622S\&C624S}$ (**E**) and Keap1$^{C613S\&C622S\&C624S}$ (**F**) MEFs were treated with 10- or 30-μM $CdCl_2$ for 3 hours.

Figure S5

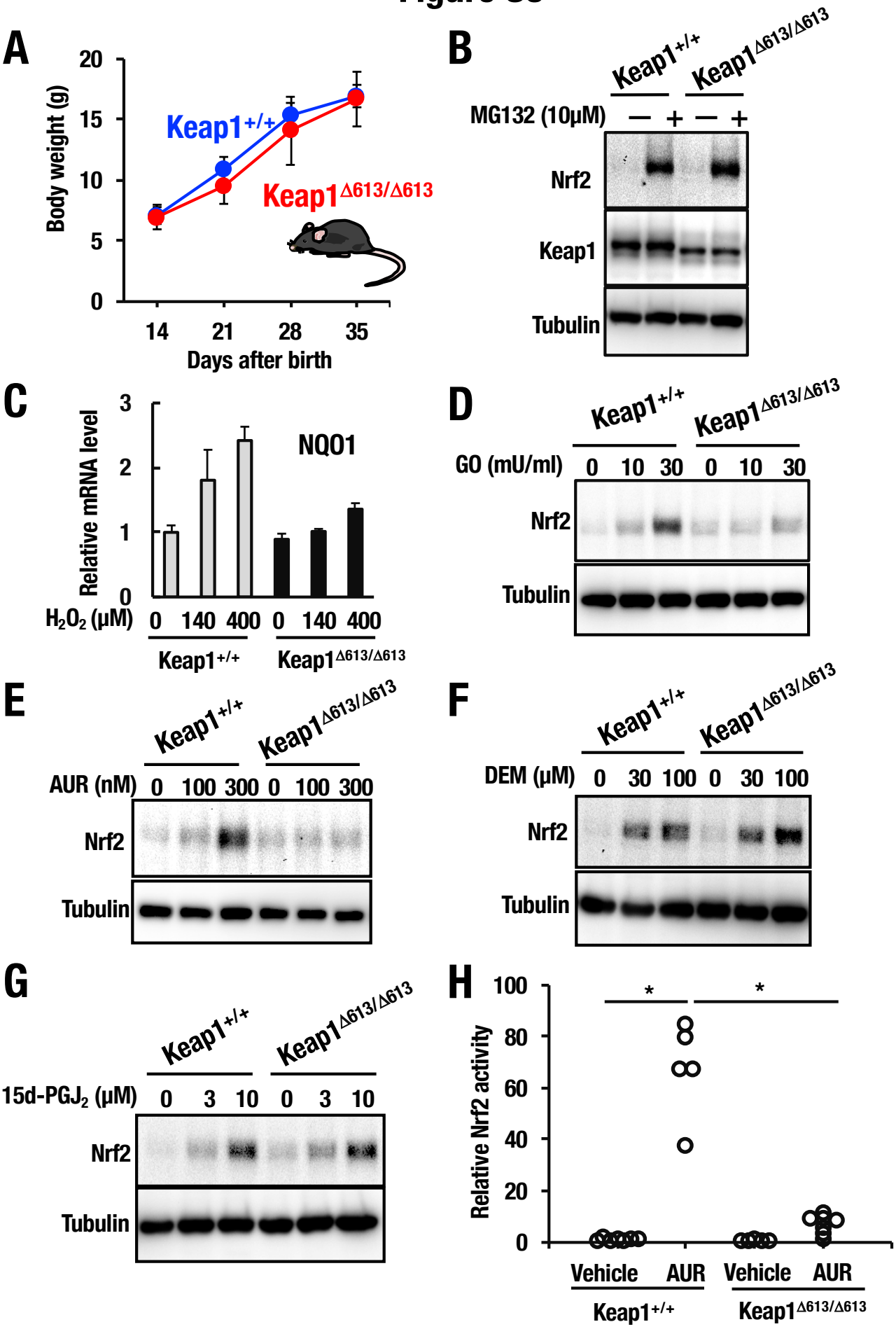
A
Body weight (g)
20
15
10
5
0
Keap1+/+
Keap1Δ613/Δ613
14
21
28
35
Days after birth
B
Keap1+/+
Keap1Δ613/Δ613
MG132 (10μM)
— + — +
Nrf2
Keap1
Tubulin
C
Relative mRNA level
3
2
1
0
NQO1
H2O2 (μM)
0 140 400 0 140 400
Keap1+/+
Keap1Δ613/Δ613
D
Keap1+/+
Keap1Δ613/Δ613
GO (mU/ml)
0 10 30 0 10 30
Nrf2
Tubulin
E
Keap1+/+
Keap1Δ613/Δ613
AUR (nM)
0 100 300 0 100 300
Nrf2
Tubulin
F
Keap1+/+
Keap1Δ613/Δ613
DEM (μM)
0 30 100 0 30 100
Nrf2
Tubulin
G
Keap1+/+
Keap1Δ613/Δ613
15d-PGJ2 (μM)
0 3 10 0 3 10
Nrf2
Tubulin
H
Relative Nrf2 activity
100
80
60
40
20
0
*
*
Vehicle
AUR
Vehicle
AUR
Keap1+/+
Keap1Δ613/Δ613

Figure S5. Cadmium is sensed by the Cys226, Cys613, and Cys622/Cys624 residues in Keap1 (Related to Figure 4). **(A)** Growth curves for Keap1+/+ and Keap1$^{\Delta 613/\Delta 613}$ mice. Note that Keap1$^{\Delta 613/\Delta 613}$ mice grew normally. Data are expressed as mean ± SE (n=3). **(B)** The ability of WT and Keap1$^{\Delta 613/\Delta 613}$ to repress Nrf2 accumulation in response to inducers was examined by Western blot. Keap1$^{+/+}$ and Keap1$^{\Delta 613/\Delta 613}$ MEFs were treated with 10-μM MG132 for 3 hours. **(C)** Keap1$^{+/+}$ and Keap1$^{\Delta 613/\Delta 613}$ MEFs were treated with 130- or 400-μM H_2O_2 for 16 hours. Expression levels of NQO1 were examined by RT-qPCR with HPRT used as an internal control. **(D-G)** The ability of WT and Keap1$^{\Delta 613/\Delta 613}$ to repress Nrf2 accumulation in response to inducers was examined by Western blot. Keap1$^{+/+}$ and Keap1$^{\Delta 613/\Delta 613}$ MEFs were treated with 10- or 30-mU/ml GO **(D)**, 100- or 300-nM AUR **(E)**, 30- or 100-μM DEM **(F)** and 3- or 10-μM 15d-PGJ_2 **(G)** for 3 hours. **(H)** Relative Nrf2 reporter activity of OKD48::Keap1$^{+/+}$ and OKD48::Keap1$^{\Delta 613/\Delta 613}$ mice treated with AUR. Mice were intraperitoneally injected with 10 mg/kg AUR, and subjected to IVIS analysis 4 hours after AUR administration. Statistically significant differences are indicated by asterisks as *$p < 0.05$. n= 5-7 per genotype.

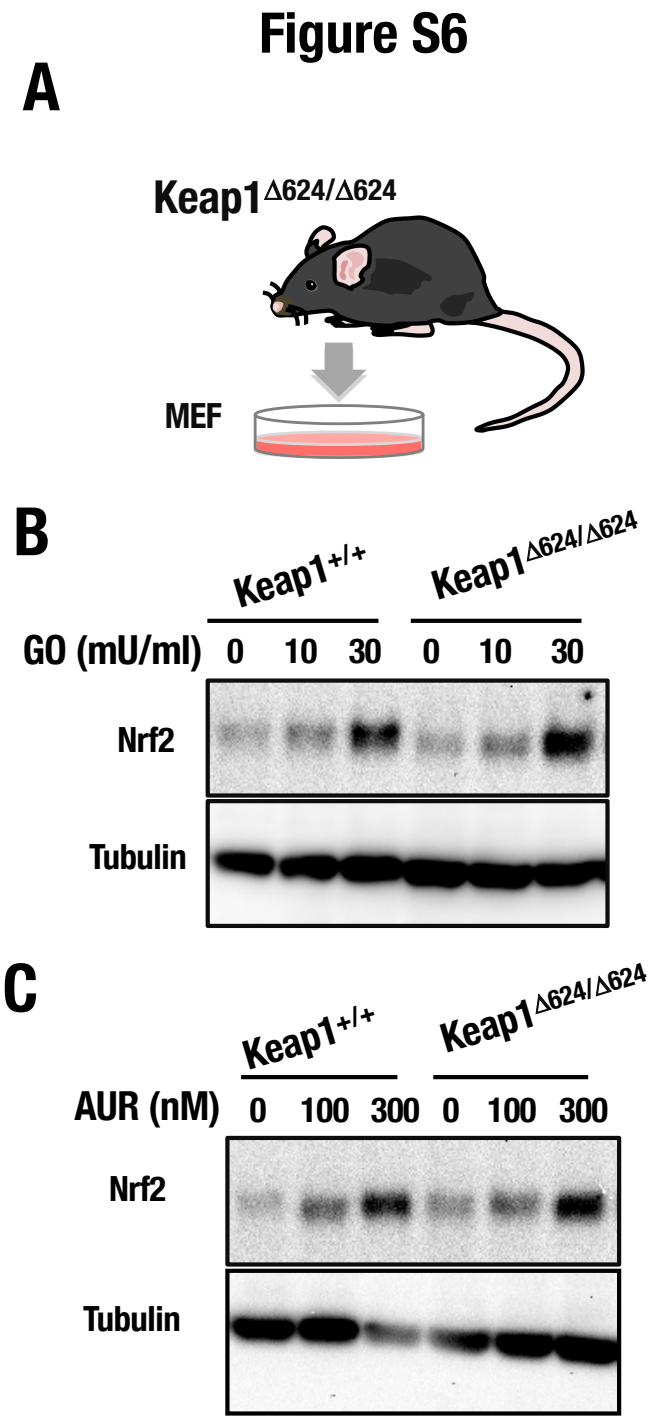

Figure S6. A single mutation in Cys624 of Keap1 is dispensable for the accumulation of Nrf2 in response to GO and AUR (Related to Figure 4).

(A) Experimental schema for preparation of MEFs from Keap1$^{\Delta 624/\Delta 624}$ mice. **(B, C)** The ability of WT and Keap1$^{\Delta 624/\Delta 624}$ to repress Nrf2 accumulation in response to inducers was examined by Western blot. Keap1$^{+/+}$ and Keap1$^{\Delta 624/\Delta 624}$ MEFs were treated with 10- or 30-mU/ml GO **(B)** and 100- or 300-nM AUR **(C)** for 3 hours.

Figure S7

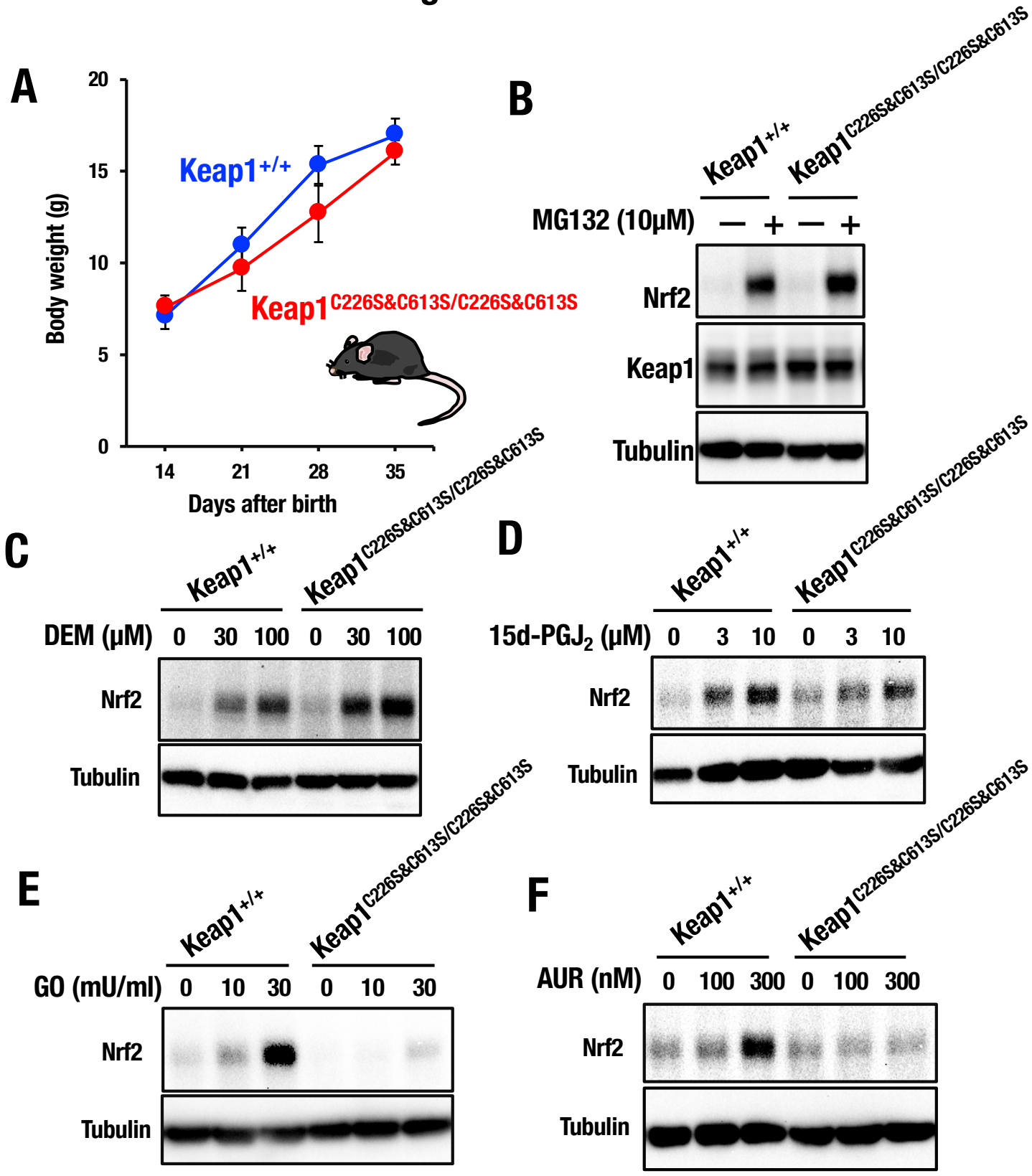

Figure S7. The combination of Cys226 and Cys613 is essential for H_2O_2-sensing but dispensable for electrophiles (Related to Figure 6)

(**A**) Growth curves for Keap1$^{+/+}$ and Keap1$^{C226S\&C613S/C226S\&C613S}$ mice. Note that Keap1$^{C226S\&C613S/C226S\&C613S}$ mice grew normally. Data are expressed as mean ± SE (n=3). **(B-F)** The ability of WT and Keap1$^{C226S\&C613S/C226S\&C613S}$ to repress Nrf2 accumulation in response to inducers was examined by Western blot. Keap1$^{+/+}$ and Keap1$^{C226S\&C613S/C226S\&C613S}$ MEFs were treated with 10-μM MG132 (**B**), 30- or 100-μM DEM (**C**), 3- or 10-μM 15d-PGJ$_2$ (**D**), 100- or 300-nM GO (**E**) and 100- or 300-nM AUR (**F**) for 3 hours.

Table S1

Keap1Cys	Inducer	Reference
C151	Sulforaphan	Hu et al, 2011
	DEM	Kobayashi et al, 2009
	DMF	Ooi et al, 2011; Adam et al, 2011
	tBHQ	Abiko et al, 2011; McMahon et al, 2010
	4-HNE, Acrolein	McMahon et al, 2010
	IAB	Eggler et al, 2005, Rachakonda et al, 2008
	Ligustilide	Dietz et al, 2008
	BMCC, XH, ISO, 10-Shogaol	Luo et al, 2007
	MeHg	Yoshida et al, 2014
C226	tBHQ	Abiko et al, 2011
	OA-NO_2	Tsujita et al, 2011; Kansanen et al, 2011
	GSSG	Holland et al, 2008
	Isoliquiritigenin	Luo et al, 2007
	NAPQI	Copple et al, 2008
C257	OA-NO_2	Kansanen et al, 2011
	Dex-Mes	Dinkova-Kostova et al, 2002
	10-Shogaol	Luo et al, 2007
	GSSG	Holland et al, 2008
C273	OA-NO2	Tsujita et al, 2011; Kansanen et al, 2011
	15d-PGJ_2, PGA_2	Kobayashi et al, 2009
	Dex-Mes	Dinkova-Kostova et al, 2002
	Ligustilide	Dietz et al, 2008
C288	DEM	Kobayashi et al, 2009
	DMF	Ooi et al, 2011; Adam et al, 2011
	OA-NO2	Kansanen et al, 2011
	4-HNE	McMahon et al, 2010
	GSSG	Holland et al, 2008
	Dex-Mes	Dinkova-Kostova et al, 2002
C319	DEM	Kobayashi et al, 2009
	XH	Luo et al, 2007
	MeHg-SG	Yoshida et al, 2014
	GSSG	Holland et al, 2008
C434	DEM	Kobayashi et al, 2009
	BMCC	Luo et al, 2007
	8-nitro-cGMP	Fujii et al, 2010
	GSSG	Holland et al, 2008
C489	Sulforaphan	Hong et al, 2005; Hu et al, 2011
	DEM, PGA_2	Kobayashi et al, 2009
	OA-NO_2	Tsujita et al, 2011; Kansanen et al, 2011
C613	DEM	Kobayashi et al, 2009
	OA-NO_2	Tsujita et al, 2011
	Dex-Mes	Dinkova-Kostova et al, 2002
	IAB	Rachakonda et al, 2008
	XH	Luo et al, 2007
	NAPQI	Copple et al, 2008
C622/624	Sulforaphan	Hong et al, 2005
	GSSG	Holland et al, 2008

Table S1. The inducer sensitivities of the 11 reactive cysteine residues reported previously (Related to Figure 1).
DEM, diethyl maleate; DMF, dimethyl fumarate; tBHQ, *tert*-butyl hydroquinone; 4-HNE, 4-hydroxy-2-nonenal; IAB, iodoacetamide biotin; BMCC, 1-biotinamido-4-(4'-[maleimidoethyl-cyclohexane]-carboxamido)butane; XH, Xanthohumol; ISO, Isoliquiritigenin; MeHg, Methylmercury; OA-NO_2; nitro oleate; GSSG, oxidized glutathione; NAPQI, N-acetyl-p-benzoquinone imine; Dex-Mes, dexamethasone 21-mesylate; 15d-PGJ_2, 15-deoxy-$D^{12,14}$-prostaglandin J_2; PGA_2, prostaglandin A_2.

Table S2 CRISPR guide sequence. Related to Star Methods.

Keap1C226	CAACCTGTCACACTGCCAGC (TGG)
Keap1C613	TTGATCAATTTGCTTCCGAC (AGG)
Keap1C622/624	ACTGTACCTGCTGAAGCACT (TGG)

Table S3 Oligonucleotides. Related to Star Methods.

Oligo	Sequence	Experiment
Keap1F14	ATCCATCGCAAACAGGGGGCTTCTTT	PCR/ sequencing
Keap1R10	CCTTCTGGTGGTGGGAGTTCAA	PCR sequencing
Keap1F20	TCCTCTCCCTTCCAAGTGAATA	PCR/ sequencing
Keap1R15	TTTCTGTCCTGTTGTCAGTGCT	PCR/ sequencing
C226S-F	CCAAGCAGGAGGAGTTCTTCAAC	Taqman/ genotyping
C226S-R	GCAGCGTACGTTCAGATCATC	Taqman/ genotyping
C226WT-P	VIC-TGTCACACTGCCAGCTG-MGB	Taqman/ genotyping
C226S-P	FAM-CTGTCACACTCCCAGCTG-MGB	Taqman/ genotyping
C613S-F	GTGAGGTGACCCGCATGAC	Taqman/ genotyping
C613S-R	TTCAGCAGGTACAGTTTTGTTGATC	Taqman/ genotyping
C613WT-P	VIC-ATGGAACCCTGTCGGAA-MGB	Taqman/ genotyping
C613S-P	FAM-ATGGAACCCTCCCGGAA-MGB	Taqman/ genotyping
d613-F	AGGTGACCCGCATGACATCT	Taqman/ genotyping
d613-R	GTCAGTGCTCAGGTATTCCAAGTG	Taqman/ genotyping
613WT-P	VIC-CCTGTCGGAAGCAA-MGB	Taqman/ genotyping
d613-P	FAM-AACCCTGAAGCAAATT-MGB	Taqman/ genotyping
d624-F	GAACCCTGTCGGAAGCAAATT	Taqman/ genotyping
d624-R	GCAGTGATACACAGACTGTTTTTCTGT	Taqman/ genotyping
624WT-P	VIC-CCTGCTGAAGCACTT-MGB	Taqman/ genotyping
d624-P	FAM-TGTACCTGAGCACTTG-MGB	Taqman/ genotyping
OKD48-F	ATCACCAGAACACTCAGTGG	PCR/ genotyping
OKD48-R	TAGCGCTTCATAGCTTCTGC	PCR/ genotyping
olMR0042	CTAGGCCACAGAATTGAAAGATCT	PCR/ genotyping
olMR0043	GTAGGTGGAAATTCTAGCATCATCC	PCR/ genotyping
NQO1-F	AGCTGGAAGCTGCAGACCTG	Taqman/ RT-qPCR
NQO1-R	CCTTTCAGAATGGCTGGCA	Taqman/ RT-qPCR
NQO1-P	ATTTCAGTTCCCATTGCAGTGGTTTGGG	Taqman/ RT-qPCR